

1 **Microbial dormancy and its impacts on Arctic terrestrial ecosystem carbon budget**

2

3 Junrong Zha and Qianlai Zhuang

4

5 Department of Earth, Atmospheric, and Planetary Sciences and Department of Agronomy,
6 Purdue University, West Lafayette, IN 47907 USA

7

8 Submitted to: *Biogeoscience*

9

10 Correspondence to: qzhuang@purdue.edu

11

12

13

14

15

16

17

18

19

20

21

22

23

24

25

26

27

28

29

30

31

32

33

34

35

36

37

38

39

40

41

42

43

44

45

46

47 **Abstract**

48 **A large amount of soil carbon in the Arctic terrestrial ecosystems could be emitted as**
49 **greenhouse gases in a warming future. However, lacking detailed microbial processes such**
50 **as microbial dormancy in current biogeochemistry models might have biased the**
51 **quantification of the regional carbon dynamics. Here the effect of microbial dormancy was**
52 **incorporated into a biogeochemistry model to improve the quantification for the last and**
53 **this century. Compared with the previous model without considering the microbial**
54 **dormancy, the new model estimated the regional soils stored 75.9 Pg more C in the**
55 **terrestrial ecosystems during the last century, and will store 50.4 Pg and 125.2 Pg more C**
56 **under the RCP 8.5 and RCP 2.6 scenarios, respectively, in this century. This study**
57 **highlights the importance of the representation of microbial dormancy in earth system**
58 **models to adequately quantify the carbon dynamics in the Arctic.**

59

60

61

62

63

64

65

66

67

68

69

70

71

72

73

74

75

76 **1. Introduction**

77 The land ecosystems in northern high latitudes (>45 °N) occupy 22% of the global
78 surface and store over 40% of the global soil organic carbon (SOC) (McGuire & Hobbie, 1997;
79 Melillo et al., 1993; Tarnocai et al., 2009; Hugelius et al., 2014). During the past decades, a
80 greening accompanying a warming in the region has been documented (Zhou et al., 2001; Lloyd
81 et al., 2002; Stow et al., 2004; Callaghan et al., 2005; Tape et al., 2006). The regional carbon
82 dynamics are expected to loom large in the global carbon cycle and exert large feedbacks to the
83 global climate system (McGuire et al., 2009; Davidson & Janssens, 2006; Bond-Lamberty &
84 Thomson, 2010).

85 To date, numerous ecosystem models have been developed to project the feedbacks
86 between terrestrial ecosystem carbon cycling and climate (Raich et al., 1991; Zhuang et al.,
87 2001, 2002, 2015; Parton et al., 1993; Knorr et al., 2005; Running & Coughlan, 1988), but they
88 can bias their quantifications due to missing detailed microbial mechanisms in these models
89 (Schmidt et al., 2011; Todd-Brown et al., 2013; Conant et al., 2011; Treseder et al., 2011).
90 Microorganisms play a central role in decomposition of litter and soil organic carbon, which
91 further governs the global carbon cycling and climate change (Xu et al., 2014; Treseder et al.,
92 2011; Wang et al., 2015). An emerging field of research has begun to incorporate microbial
93 ecology into existing process-based models to represent decomposition in ways that include
94 important microbial processes that were previously ignored (Zha & Zhuang, 2018; Schimel &
95 Weintraub, 2003; Allison et al., 2010; German et al., 2012). These microbial-based models tend
96 to better reproduce field and satellite observations than traditional ones that treat soil
97 decomposition as a first-order decay process without considering microbial activities (Treseder
98 et al., 2011; Wieder et al., 2013; Todd-Brown et al., 2011; Lawrence et al., 2009; Moorhead et

99 al., 2006). However, some vital microbial traits such as microbial dormancy and community
100 shifts are still rarely explicitly considered in large-scale ecosystem models (Wieder et al., 2015),
101 and this may introduce notable uncertainties (Graham et al., 2014, 2016; Wang et al., 2015;
102 Bouskill et al., 2012; Kaiser et al., 2014).

103 Dormancy is broadly recognized as a strategy for microorganisms to cope with periodical
104 environmental stresses (Harder & Dijkhuizen, 1983). When environmental conditions are
105 unfavorable for growth, microbes switch to a dormant state, which is a reversible state of low to
106 zero metabolic activity (Stolpovsky et al., 2011; Lennon & Jones, 2011). In this state,
107 biogeochemical processes such as soil decomposition are slow (Blagodatskaya et al., 2013). At
108 any given time, there is only a fraction of, likely below 50%, metabolically active microbes in
109 natural soils (Wang et al., 2015; Stolpovsky et al., 2011). Soil decomposition and nutrient
110 cycling mainly depend on these active microbes because only active ones can consume organic
111 matter and replicate themselves (Wang et al., 2015; Blagodatskaya et al., 2014). To date, most
112 existing biogeochemistry models use total rather than active microbial biomass as an indicator of
113 microbial activities (Wieder et al., 2015), which could bias the estimates of soil decomposition
114 and ecosystem carbon budget (Hagerty et al., 2014; He et al., 2015). Especially, the Arctic
115 terrestrial ecosystems are nitrogen-limited, neglecting microbial dormancy will lead to incorrect
116 estimates of nitrogen availability through soil decomposition, failing to capture nitrogen
117 feedbacks to carbon dynamics (Wang et al., 2015; Stolpovsky et al., 2011; Thullner et al., 2005).
118 Furthermore, the Arctic has experienced a marked seasonality of active and dormant microbial
119 cycles and the above-global-average warming, which might have increased the proportion of
120 active microbes in soils (He et al., 2015). Thus, incorporating dormancy effects will improve
121 model realism to provide a better projection of the Arctic carbon dynamics.

122 This study incorporated the effects of microbial dormancy trait into an extant process-
123 based biogeochemistry model (MIC-TEM) (Zha & Zhuang, 2018; He et al., 2015). The dormant
124 and active microbial physiology has been considered explicitly in the new version of model
125 (MIC-TEM-dormancy). The revised model was parameterized, validated, and then applied to
126 evaluate the carbon dynamics during the last and this centuries in the Arctic terrestrial
127 ecosystems (north 45 °N above). By comparing the results of MIC-TEM-dormancy and MIC-
128 TEM, we can show that incorporating microbial dormancy may produce a much different
129 prediction in historical and future carbon budget.

130

131 **2. Methods**

132 **2.1 Overview**

133 Due to the importance of microbial dormancy, some recent work has been done to consider
134 the metabolic activation and deactivation of microbes in soil and its effects on soil carbon (C)
135 dynamics and climate feedbacks. For example, Wang et al. (2015) has incorporated transformation
136 processes between active and dormant states to develop two versions of MEND, that is, MEND
137 with and without dormancy. The two versions of the model have been applied to quantify the
138 carbon decomposition in laboratory incubations of four soils. Salazar et al. (2018) have also taken
139 microbial dormancy into account to compare their predictions of microbial biomass and soil
140 heterotrophic respiration (R_H) under simulated cycles of stressful (dryness) and favorable (wet
141 pulses) conditions. Our study extends those modeling studies to the whole Arctic region by
142 developing a more detailed biogeochemistry model considering the dormancy impacts. Below, we
143 first describe how we developed the new model (MIC-TEM-dormancy) by incorporating the
144 microbial dormancy trait into an existing microbial-based biogeochemistry model (MIC-TEM).

145 Second, we discuss how parameterization and validation of MIC-TEM-dormancy model were
146 conducted using observed net ecosystem exchange data, and heterotrophic respiration data at
147 representative sites. Third, we presented how the model was applied to northern high latitudes
148 (above 45 °N) for the 20th and 21st centuries and discussed the dormancy effects on regional carbon
149 budget.

150

151 **2.2 Model description**

152 A non-dormancy version of biogeochemistry model (MIC-TEM) has been developed by
153 incorporating a microbial module (Allison et al., 2010) into an extant large-scale biogeochemical
154 model (TEM) to explicitly (Zhuang et al., 2003) consider the effects of microbial dynamics and
155 enzyme kinetics on carbon dynamics (Zha & Zhuang, 2018). Here we further advanced the MIC-
156 TEM by incorporating algorithms that describe the effects of microbial dormancy dynamics
157 based on He et al. (2015). Different from He et al. (2015), in which microbial module was driven
158 with existing data of carbon stocks and fluxes, our study incorporated the microbial module into
159 an extant MIC-TEM that simulates carbon data dynamically. This coupling enables us to
160 extrapolate our model to whole northern high-latitudes region, rather than only for temperate
161 forest region in He et al. (2015). In our new model (MIC-TEM-dormancy), microbial biomass
162 pool was divided into two fractions, including the dormant and active microbial biomass pools.
163 The two microbial biomass pools and the reversible transition between them have been
164 considered explicitly in the new model (Figure 1), which was ignored in MIC-TEM.

165 In previous MIC-TEM, heterotrophic respiration (R_H) is calculated as:

$$166 \quad R_H = \text{ASSIM} \times (1 - \text{CUE}) \quad (1)$$

167 Where ASSIM and CUE represent microbial assimilation and carbon use efficiency, respectively.
 168 For detailed carbon dynamics in MIC-TEM, see Zha & Zhuang (2018).

169 Here we revised MIC-TEM by incorporating microbial dormancy dynamics according to
 170 He et al. (2015). In MIC-TEM-dormancy, the soil heterotrophic respiration R_H is comprised of
 171 three parts: the maintenance respiration from the active and dormant microorganisms and the CO_2
 172 production through the process of microbial assimilation (He et al., 2015):

$$173 \quad R_H = m_R Q_{10mic}^{\frac{temp-15}{10}} B_a + \beta m_R Q_{10mic}^{\frac{temp-15}{10}} B_d + CO_2 \quad (2)$$

174 where the first two terms are maintenance respiration from the active and dormant
 175 microorganisms, respectively. The last term is the CO_2 produced during the process of microbial
 176 assimilation.

177 For first two terms, B_a and B_d represents the active and dormant microbial biomass pool,
 178 respectively. The parameter m_R denotes the specific maintenance rate at active state (h^{-1}), and β
 179 is the ratio of dormant maintenance rate to active maintenance rate. Thus, βm_R denotes the
 180 maximum specific maintenance rate at dormant state. Temperature sensitivity was expressed as
 181 the Q_{10} function ($Q_{10}^{\frac{temp-15}{10}}$), where temp is soil temperature at top 20 cm (units: $^{\circ}C$).

182 For the third term, the CO_2 produced through microbial assimilation is calculated as in He et al.
 183 (2015) and Allison et al. (2010):

$$184 \quad CO_2 = ASSIM \times (1 - Y_g) \quad (3)$$

185 Where ASSIM represents the microbial assimilation and the parameter Y_g represents carbon use
 186 efficiency. Microbial assimilation (ASSIM) is calculated as in He et al. (2015):

$$187 \quad ASSIM = \frac{1}{Y_g} \frac{\Phi}{\alpha} m_R Q_{10enz}^{\frac{temp-15}{10}} B_a \left(\frac{CN_{soil}}{CN_{mic}} \right)^{0.6} \quad (4)$$

188 Here parameter α is maintenance weight (h^{-1}), CN_{soil} and CN_{mic} denotes the C:N ratios of soil and
 189 that of microbial biomass. Besides, Φ is the substrate saturation level and defined as in He et al.
 190 (2015) and Wang et al. (2014):

$$191 \quad \Phi = \frac{S}{K_s + S} \quad (5)$$

192 Where K_s is the half saturation constant for substrate uptake as indicated by the Michaelis–Menten
 193 kinetic, and S is soluble C substrates that are directly accessible for microbial assimilation (Wang
 194 et al., 2014). Here we quantified concentration of soluble C substrates that are directly accessible
 195 for microbial assimilation by using conceptual framework from Davidson et al. (2012):

$$196 \quad S = \text{Soluble C} \times D_{liq} \times \theta^3 \quad (6)$$

197 The term ‘Soluble C’ denotes the state variable of soluble carbon pool. D_{liq} is the diffusion
 198 coefficient of the substrate in the liquid phase, and is formulated as:

$$199 \quad D_{liq} = 1/(1-BD/PD)^3 \quad (7)$$

200 Where BD is the bulk density and PD is the soil particle density. θ is the volumetric soil moisture.
 201 Different from MIC-TEM, the transitions between active and dormant microbial biomass are
 202 included in MIC-TEM-dormancy.

$$203 \quad B_{a \rightarrow d} = (1 - \Phi) m_R Q_{10mic}^{\frac{temp-15}{10}} B_a \quad (8)$$

$$204 \quad B_{d \rightarrow a} = \Phi m_R Q_{10mic}^{\frac{temp-15}{10}} B_d \quad (9)$$

205 Where $B_{a \rightarrow d}$ and $B_{d \rightarrow a}$ denote the transition from the active to dormant microbe and from the
 206 dormant to active microbe, respectively (He et al., 2015; Wang et al., 2014). Thus, dormancy rate
 207 is affected by active and dormant biomass, soil temperature ($temp$) and soil moisture (θ in Φ).

208 The active microbial biomass (B_a) is modeled as (He et al., 2015; Wang et al., 2014):

$$209 \quad \frac{dB_a}{dt} = \text{ASSIM} \times Y_g - m_R Q_{10mic}^{\frac{temp-15}{10}} B_a - B_{a \rightarrow d} + B_{d \rightarrow a} - \text{DEATH} - \text{EPROD} \quad (10)$$

210 Where DEATH and EPROD denotes microbial biomass death and enzyme production, which are
 211 modeled as proportional to active microbial biomass with constant rates r_{death} and r_{EnzProd} (Allison
 212 et al., 2010):

$$213 \quad \text{DEATH} = r_{\text{death}} \times \text{Ba} \quad (11)$$

$$214 \quad \text{EPROD} = r_{\text{EnzProd}} \times \text{Ba} \quad (12)$$

215 Where r_{death} and r_{EnzProd} are the rate constants of microbial death and enzyme production,
 216 respectively.

217 The dormant microbial biomass (B_d) is modeled as (He et al., 2015; Wang et al., 2014):

$$218 \quad \frac{dB_d}{dt} = -\beta m_R Q_{10\text{mic}}^{\frac{\text{temp}-15}{10}} B_d + B_{a \rightarrow d} - B_{d \rightarrow a} \quad (13)$$

219 The Soluble C pool is modeled as (He et al., 2015; Allison et al., 2010):

$$220 \quad \frac{d \text{Soluble C}}{dt} = \text{DECAY} - \text{ASSIM} + \text{ELOSS} + \text{DEATH} \quad (14)$$

221 Where DECAY represents the enzymatic decay of soil organic carbon (SOC), and ELOSS
 222 represents the loss of enzyme.

223 DECAY is regulated by enzyme biomass (ENZ), soil organic carbon (SOC), soil temperature, and
 224 substrate quality (He et al., 2015):

$$225 \quad \text{DECAY} = V_{\text{max}} \times Q_{10\text{enz}}^{\frac{\text{temp}-15}{10}} \times \text{ENZ} \times \frac{\text{SOC}}{K_{m\text{uptake}} + \text{SOC}} \times (120 - \text{CN}_{\text{soil}}) \quad (15)$$

226 Where V_{max} is the maximum SOC decay rate, $K_{m\text{uptake}}$ is half saturation constant for enzymatic
 227 decay.

228 ELOSS is modeled as a first-order process (Allison et al., 2010) to represent enzyme turnover:

$$229 \quad \text{ELOSS} = r_{\text{enzloss}} \times \text{ENZ} \quad (16)$$

230 Where r_{enzloss} is the rate constant of enzyme loss.

231 The soil organic carbon pool (SOC) is modeled as:

232
$$\frac{dSOC}{dt} = \text{Litterfall} - \text{DECAY} \quad (17)$$

233 Where Litterfall is estimated as a function of vegetation carbon (Zhuang et al., 2010).

234 Last, enzyme pool (ENZ) is modeled as:

235
$$\frac{dENZ}{dt} = \text{EPROD} - \text{ELOSS} \quad (18)$$

236 With the modification of microbial carbon dynamics by considering microbial life-history trait,
237 soil decomposition is changed since it is controlled by microbes. When microbial dormancy is
238 considered, the number of active microbes that participate in soil decomposition is much less. The
239 changes in soil decomposition directly influence the amount of soil respiration, and further
240 influence soil nitrogen (N) mineralization that determines soil N availability for plants, affecting
241 gross primary production (GPP). Since both GPP and R_H can be affected by microbial dormancy,
242 net ecosystem production (NEP) will also be affected.

243

244 **2.3 Model parameterization and validation**

245 The detailed description of parameters that are related to microbial dormancy can be found
246 in He et al. (2015) (Table 1). Here we calibrated the MIC-TEM-dormancy at six representative
247 sites with gap-filled monthly net ecosystem productivity (NEP, $\text{gCm}^{-2}\text{mon}^{-1}$) data in northern high
248 latitudes (Table 2). Site-level climatic data and soil texture data were organized for driving model.
249 All sites information can be found on AmeriFlux network (Davidson et al., 2000). The results for
250 model parameterization were presented in Figure 2. We conducted the parameterization using a
251 global optimization algorithm known as SCE-UA (Shuffled complex evolution) method (Duan et
252 al., 1994). An ensemble of 50 independent sets of parameters were performed based on prior ranges
253 from literature (Table 1) to minimize the difference between the monthly simulated and measured
254 NEP at the chosen sites. The cost function of the minimization is:

255
$$\text{Obj} = \sum_{i=1}^k (\text{NEP}_{\text{obs},i} - \text{NEP}_{\text{sim},i})^2 \quad (17)$$

256 Where $\text{NEP}_{\text{obs},i}$ and $\text{NEP}_{\text{sim},i}$ are the observed and simulated NEP, respectively. k is the number of
257 data pairs for comparison. Except for the parameters of microbial dormancy, other parameters are
258 derived directly from MIC-TEM (Zha & Zhuang, 2018). The optimized parameters were used for
259 model validation and regional simulations.

260 For model validation, we chose another six sites that containing monthly NEP data from
261 AmeriFlux network (Table 3). Moreover, we also conducted site-level validations with monthly
262 soil respiration data from AmeriFlux network and Fluxnet dataset. The site information was
263 provided in Table 4. For these sites, we assumed 50% of soil respiration was heterotrophic
264 respiration (R_H) for forest (Hanson et al., 2000), 60% and 70% of that was R_H for grassland (Wang
265 et al., 2009) and tundra (Billings et al., 1977). Because there is a limited amount of available R_H
266 data, we could not conduct a regional validation for all pixels in northern high latitudes. Instead,
267 we extracted 61 sites providing data of average annual heterotrophic respiration from ORNL global
268 Soil Respiration Dataset (https://daac.ornl.gov/SOILS/guides/SRDB_V4.html, Bond-Lamberty et
269 al., 2018) for model validation. The site-level observed average annual R_H was used to compare
270 with simulated annual R_H by MIC-TEM-dormancy and MIC-TEM. The MIC-TEM-dormancy was
271 run at monthly time step to keep consistent with the time step of MIC-TEM. Although microbial
272 dynamics occur at fine temporal scales (Tang & Riley, 2014), we can still quantify the cumulative
273 impacts of microbial dynamics on carbon and nitrogen cycling at monthly time by not changing
274 the model structure.

275

276 **2.4 Spatial extrapolation**

277 For historical simulations during the 20th century, two sets of regional simulations using
278 MIC-TEM-dormancy and MIC-TEM at a spatial resolution of 0.5° latitude × 0.5° longitude were
279 conducted. Our model simulation contains two parts: spin-up and transient simulation. A typical
280 spin-up was conducted to get the model to a steady state for each spatial location, which will be
281 used as initial conditions for transient simulations (McGuire et al., 1992). During spin-up
282 procedure, cyclic forcing data was used to force the model run, and repeated continuously until
283 dynamic equilibrium was achieved at which the modeled state variables show a cyclic pattern or
284 become constant. Specifically, this study used the monthly historical climate data from 1900 to
285 1940 to repeatedly drive the model for the spin-up. Before spin-up procedure, the model was
286 initialized with default built-in carbon stocks (Raich et al., 1991). During transient simulations,
287 the calibrated ecosystem-specific parameters were used for regional simulations. The previous
288 dynamic equilibrium was used as initial value for transient simulation. The historical climatic
289 forcing data, including the monthly air temperature, precipitation, cloudiness, and atmospheric
290 CO₂ concentrations, were organized from the Climatic Research Unit (CRU TS3.1) from the
291 University of East Anglia (Harris et al., 2014). We also used gridded data of soil texture (Zhuang
292 et al., 2003), elevation (Zhuang et al., 2015), and potential natural vegetation (Melillo et al., 1993)
293 from literatures. In our model, we assumed that soil texture, elevation, and potential natural
294 vegetation data only vary spatially, not vary over time (Zhuang et al., 2015).

295 In addition, regional simulations over the 21st century were conducted under two
296 Intergovernmental Panel on Climate Change (IPCC) climate scenarios (RCP 2.6 and RCP 8.5).
297 The future climatic forcing data under these two climate change scenarios were derived from the
298 HadGEM2-ESmodel, which is a member of CMIP5project213 ([https://esgf-](https://esgf-node.llnl.gov/search/cmip5/)
299 [node.llnl.gov/search/cmip5/](https://esgf-node.llnl.gov/search/cmip5/)). Then the regional estimations were obtained by summing up the

300 gridded outputs for our study region. The positive simulated NEP represents a CO₂ sink from the
301 atmosphere to terrestrial ecosystems, while a negative value represents a source of CO₂ from
302 terrestrial ecosystems to the atmosphere.

303 **2.5 Parameter equifinality effects**

304 Our previous studies using TEM has demonstrated that equifinality derived from site-level
305 parameterization will affect the uncertainty in the estimation of regional carbon dynamics (Tang
306 and Zhuang, 2008, 2009). Here equifinality refers to that a number of sets of parameters result in
307 model simulations that all match the data similarly well. To quantify this effect on our simulation
308 uncertainty, we conducted ensemble regional simulations with 50 sets of parameters for both
309 historical and future studies. The 50 sets of parameters were obtained according to the method in
310 Tang and Zhuang (2008).

311 **3. Results**

312 **3.1 Inversed Model Parameters and model validation**

313 Using SCE-UA ensemble method, 50 independent sets of parameters were converged to
314 minimize the objective function. Then the optimized parameters are calculated as the mean of these
315 50 sets of inversed parameters. The boxplot of parameter posterior distributions reflects different
316 ecosystem properties at these sites (Figure 3). For instance, growth yield was higher in tundra types
317 than in forests, meaning microorganisms in environment with higher energy limitation tend to
318 enhance the efficiency of energy transportation. Besides, alpha, the maintenance weight, was also
319 higher in tundra types than in forests. From the plot for parameter beta, the ratio of dormant
320 maintenance rate to specific maintenance rate for active biomass in tundra types is lower than that
321 in forest types. Other microbial related parameters did not differentiate much among different
322 vegetation types.

323 After parameterization, the MIC-TEM-dormancy was validated with monthly NEP data for
324 six representative ecosystems, and the comparisons between monthly observed NEP and
325 simulated NEP were presented in Figure 4. With the optimized parameters, the dormancy-based
326 model was used to reproduce NEP to compare with the measured NEP (Table 5). The R^2 ranges
327 from 0.67 for Atqasuk to 0.93 for Bartlett Experimental Forest (Table 5). Generally, our new
328 model performs better for forest ecosystems than for tundra ecosystems. Compared with MIC-
329 TEM, dormancy model performs better for alpine tundra, temperate coniferous forest, and
330 grassland. For other sites, both models show similar performance (Table 5). Besides, a set of
331 monthly soil respiration data were selected to evaluate the estimated R_H . The comparisons
332 between monthly observed R_H and simulated R_H from two contrasting models were conducted
333 (Figure 5). MIC-TEM-dormancy has higher R^2 and lower root mean square error (RMSE) (Table
334 6). Sixty-one sites with average annual R_H in northern high-latitude regions were used to further
335 evaluate the new model performance. The dormancy model has lower intercept and slope with R^2
336 of 0.45, while R^2 of MIC-TEM is 0.3 (Figure 6). These analyses indicate that new model is more
337 realistic in representing R_H by considering microbial dormancy. This difference in R_H further
338 affects soil available nitrogen dynamics, influencing nitrogen uptake by plants, the rate of
339 photosynthesis and NPP (Zhuang et al., 2015; Zha et al., 2018; Thullner et al., 2005).

340

341 **3.2 Regional carbon dynamics during the 20th century**

342 Regional extrapolation with both models estimated a regional carbon sink but with different
343 magnitudes (Figure 7c). With optimized parameters, MIC-TEM estimated a regional carbon sink
344 of 77.6 Pg with the interannual standard deviation of 0.21 Pg C yr⁻¹ during the 20th century.
345 However, MIC-TEM-dormancy nearly doubles the sink at 153.5 Pg with the interannual standard

346 deviation of $0.12 \text{ Pg C yr}^{-1}$ during the last century (Figure 7c). At the end of the century, MIC-
347 TEM estimated that NEP reaches 1.0 Pg C yr^{-1} in comparison with MIC-TEM-dormancy estimates
348 of 1.5 Pg C yr^{-1} (Figure 7c). Both models simulated similar trends for regional NPP, R_H and NEP
349 (Figure 7). Generally, they show an increasing trend in the 20th century (Figure 7). Meanwhile,
350 with optimized parameters, MIC-TEM-dormancy estimated NPP and R_H at $7.94 \text{ Pg C yr}^{-1}$ and 6.4
351 Pg C yr^{-1} , which are 5.8% and 16.3% less than the estimations from MIC-TEM, respectively
352 (Figures 7a and 7b). This pronounced difference of NEP between two models comes from the
353 disparity between the simulated NPP and R_H with them since NEP is calculated as the difference
354 between NPP and R_H . Without considering dormancy, MIC-TEM estimates more active microbial
355 biomass since it assumes the whole microbial biomass pool will participate in soil decomposition.
356 The fact is only active part of microbial biomass can affect organic matter decomposition, meaning
357 MIC-TEM overestimates R_H . On the other hand, overestimation of R_H can induce higher nitrogen
358 uptake by plants, which will accelerate rate of photosynthesis and further enhance NPP projection.
359 Although MIC-TEM estimates higher NPP and R_H than MIC-TEM-dormancy does, NEP estimated
360 from MIC-TEM is actually lower.

361 The average annual seasonal patterns of NPP, R_H and NEP during the 1990s were also
362 organized from regional simulations with two models (Figure 8). Temporally, both models
363 projected higher NPP and R_H in summer than in winter (Figures 8a and 8b) due to higher soil
364 temperature and moisture (McGuire et al., 1992). Setting the R_H projection from MIC-TEM as a
365 baseline, MIC-TEM-dormancy averagely projected 33% less R_H in summer (May to September),
366 and 30% more in winter (other months) (Figure 8b), which indicates that without dormancy,
367 model tends to estimate lower soil respiration compared to dormancy model due to ignorance of
368 dormant respiration in winter but estimate higher soil respiration due to higher estimation of

369 active biomass in summer. In the meantime, seasonal cycle of NPP with MIC-TEM-dormancy
370 shows a relative flattening pattern compared with MIC-TEM, which is similar to seasonal cycle
371 of R_H (Figure 8a). Though R_H and NPP show the similar seasonal patterns, NEP can still show
372 different pattern. Here seasonal cycles of NEP with models are close to each other (Figure 8c),
373 but dormancy model projected slightly higher NEP in summer.

374 **3.3 Regional carbon dynamics during the 21st century**

375 Under the RCP 8.5 scenario, both models estimated the region acts as a carbon sink (Figure
376 9). The MIC-TEM-dormancy predicted a C accumulation of 129.9 Pg by the end of this century.
377 with the interannual standard deviation of 0.13 Pg C yr⁻¹, whereas MIC-TEM estimates a C
378 accumulation of 79.5 Pg with the interannual standard deviation of 0.37 Pg C yr⁻¹ during the 21st
379 century (Figure 9). Thus, MIC-TEM-dormancy estimates an increase of 50.4 Pg regional carbon
380 sequestration relative to MIC-TEM, with less interannual variation (Figure 9). Under this
381 scenario, both models predict similar temporal trends for NEP, namely increasing from the 2000s
382 and then decreasing from the 2070s onward (Figure 9). MIC-TEM-dormancy predicts that
383 carbon sink reaches 1.36 Pg C yr⁻¹ in the 2090s, which is 0.26 Pg C yr⁻¹ more than projection of
384 MIC-TEM. Moreover, MIC-TEM-dormancy estimated NPP and R_H at 10.2 Pg C yr⁻¹ and 8.9 Pg
385 C yr⁻¹, which are 1.3 Pg C yr⁻¹ and 1.8 Pg C yr⁻¹ less than the estimations from MIC-TEM,
386 respectively (Figure 9).

387 Under the RCP 2.6 scenario, the cumulative NEP from two models diverged by 125.2 Pg C
388 by 2100. The trajectory of inter-annual NEP estimated with the two models also diverged. The
389 MIC-TEM predicted the region fluctuates between carbon sinks and sources, and totally acts as a
390 carbon source of 1.6 Pg C with the interannual standard deviation of 0.24 Pg C yr⁻¹ during the
391 21st century. In contrast, MIC-TEM-dormancy projected the region acts as a carbon sink of 123.6

392 Pg C with an interannual standard deviation of 0.1 Pg C yr⁻¹ (Figure 9). MIC-TEM-dormancy
393 estimates NPP and R_H at 9.9 Pg C yr⁻¹ and 8.7 Pg C yr⁻¹, which are 0.5 Pg C yr⁻¹ and 1.7 Pg C yr⁻¹
394 ¹ less than the estimations from MIC-TEM, respectively (Figure 9). Moreover, simulations under
395 the two contrasting climate scenarios (RCP 2.6 and RCP 8.5) exhibit a large difference of 81.1
396 Pg C of cumulative NEP during the 21st century by MIC-TEM, but only 6.3 Pg C of that by
397 MIC-TEM-dormancy. This difference indicates microbes provide a resistant response to climate
398 change due to dormancy to some extent (Treseder et al., 2011).

399 The average annual seasonal patterns of NPP, R_H and NEP during the 2990s by two
400 models were also presented (Figure 10). MIC-TEM-dormancy estimated higher R_H in winter, but
401 lower R_H in summer under both future scenarios (Figure 10). NPP is the same in winter with or
402 without dormancy, and in the late summer is higher than that without dormancy, especially in the
403 RCP 8.5 scenario. The combined flattening patterns of NPP and R_H result in different patterns
404 for NEP. Under the RCP 2.6 scenario, MIC-TEM-dormancy predicts higher NEP from June to
405 October, but lower NEP from January to April compared to MIC-TEM (Figure 10). Under the
406 RCP 8.5 scenario, MIC-TEM-dormancy predicts higher NEP from June to September, but much
407 lower NEP in other months than MIC-TEM (Figure 10).

408 **3.4 Regional uncertainty considering equifinality effects during 20th and 21st centuries**

409 The ensemble simulations for the 20th century is shown in Figure 11. Given the
410 uncertainty in parameters, MIC-TEM-dormancy predicted that the regional cumulative carbon
411 ranges from a carbon loss of 28.2 Pg to a carbon sink of 362.1 Pg by different ensemble
412 members, with a mean of 71.2±54.8 Pg (Figure 11). For the 21st century, MIC-TEM-dormancy
413 predicted that the region acts from a carbon source of 49.3 Pg C to a carbon sink of 296.5 Pg C,
414 with a mean of 112.7±116.5 Pg under the RCP 2.6 scenario (Figure 12). Under the RCP 8.5

415 scenario, MIC-TEM-dormancy predicted that the region acts from a carbon source of 27.1 Pg C
416 to a carbon sink of 401.3 Pg C, with a mean of 143.1 ± 162.5 Pg (Figure 12).

417 **4. Discussion**

418 Soils are the largest carbon repository in the terrestrial biosphere and hold 2.5 times more
419 carbon than the atmosphere (Frey et al., 2013; Schlesinger & Andrews, 2000). Especially, a
420 significant portion of soil organic carbon stored in northern high latitudes (Tarnocai et al., 2009).
421 Besides, the magnitude of the warming in these regions is larger, almost twice, that of the global
422 average (Serreze & Francis, 2006) and the changing climate is expected to alter the carbon cycle
423 through influencing the activities of microorganisms in controlling soil decomposition (Manzoni
424 et al., 2012; Melillo et al., 2011). Therefore, explicit consideration of microbial traits and
425 functions in large-scale biogeochemistry models is necessary for better quantification of carbon-
426 climate feedbacks (Thullner et al., 2005; Wang et al., 2015). Our regional simulations with two
427 contrasting models (MIC-TEM, MIC-TEM-dormancy) indicate the region was a carbon sink in
428 past decades, which is consistent with results from other process-based models (White et al.,
429 2000; Houghton et al., 2007; McGuire et al., 2009; Schimel, 2013). However, the magnitudes of
430 this sink are quite different in two models. Moreover, MIC-TEM-dormancy predicts the sink will
431 decrease under both RCP 8.5 and RCP 2.6 scenarios during the 21st century, while MIC-TEM
432 projects that the sink will increase under the RCP 8.5 but change to carbon source under the RCP
433 2.6 scenario. Estimations based on models without dormancy could fit observations of R_H as well
434 as estimations with dormancy, but at the cost of underestimating microbial biomass (Wang et al.,
435 2014). Differences in predicted R_H with and without dormancy increase with temperature and
436 with the length of the dry periods between wetting events (Salazar et al., 2018). The large
437 difference in two models suggests the importance of incorporating microbial dormancy effects.

438 The large bias between dormancy and non-dormancy models mainly comes from two parts.
439 First, many important microbial activities such as soil organic carbon decomposition and nutrient
440 cycling largely depend on the active fraction of microbial communities, not total microbial
441 biomass (Wang et al., 2014; Blagodatsky et al., 2000). However, only a small part (about 0.1-
442 2%, seldom exceed 5%) of the total soil microbial biomass is recognized to be active under
443 natural conditions (Blagodatsky et al., 2011; Werf & Verstraete, 1987). Thus, dormancy could be
444 a prominent feature in soil systems (Wang et al., 2014). Without considering dormancy, the
445 “effective” microbial biomass for soil decomposition could be overestimated, resulting in
446 overestimation of heterotrophic respiration (He et al., 2015). He et al. (2015) predicted total soil
447 R_H of all temperate forests (25°N-50°N) from the dormancy model amounted to 7.28 Pg C yr⁻¹
448 and 8.83 Pg C yr⁻¹ from a no-dormancy model, which is 21.3% higher than the dormancy model.
449 Although their study region and simulation period are different from our study, the results can
450 still be comparable. Both studies indicated that the magnitude of R_H from no-dormancy model
451 are higher than dormancy models. Second, high soil respiration stimulates N mineralization in
452 soils (Zhuang et al., 2001, 2002), making more nutrients for photosynthesis of plants (Raich et
453 al., 1991; McGuire et al., 1995). Therefore, NPP will be higher due to the N enrichment from
454 higher R_H . However, how NEP will change is still unclear. Our estimates of the northern
455 extratropical NEP in the 1980s (1.61 Pg C yr⁻¹ with MIC-TEM-dormancy and 0.84 Pg C yr⁻¹
456 with MIC-TEM) are within ranges (0.6 to 2.3 PgC yr⁻¹) reported in the literature for northern
457 regions (Schimel et al., 2001). Moreover, our predicted time trajectory of NEP in the 21st
458 century under the RCP 2.6 scenario is very similar to the finding of White et al. (2000),
459 indicating that NEP increases from the 2000s to the 2070s, and then decreases in the 2090s.
460 Although our dormancy model can project reasonable carbon fluxes and indicate the importance

461 of incorporating microbial dormancy when compared with MIC-TEM (Zha & Zhuang et al.,
462 2018), there are some other microbial traits have not yet been considered in our model. For
463 instance, one vital common evolutionary trait of microbe is the community shift (Wang et al.,
464 2015) with changing environment, including warming, N fertilization and precipitation (Treseder
465 et al., 2011; Frey et al., 2013; Allison et al., 2009; Evans & Wallenstein, 2011). Community shift
466 will influence microbial physiology, temperature sensitivity and growth rates (Classen et al.,
467 2015), which will further affect the rate of soil decomposition and other carbon dynamics
468 (Treseder et al., 2011; Schimel & Schaeffer, 2012; Todd-Brown et al., 2011). Besides, microbial
469 community composition was ignored in our model. We didn't separate among functional
470 microbial groups, but gather microbes into one "box". However, microbial community
471 composition could influence ecosystem functioning, and their variance in responses to
472 environmental conditions could alter the prediction of the rates of decomposition of organic
473 material (Balser et al. 2002; Fierer et al. 2007). Especially, some narrowly-distributed functions
474 can be more sensitive to microbial community composition, and these might benefit most from
475 explicit consideration of distinguishing functional groups in ecosystem models (McGuire &
476 Treseder, 2010; Schimel 1995). Thus, functional dissimilarity in microbial communities can be
477 considered in next step for model development (Strickland et al., 2009; Moorhead et al., 2006).
478 Moreover, microbial acclimation, a mechanism of adaption to a new temperature regime, is
479 another important trait to affect soil decomposition. Recent studies have found that the warming-
480 induced elevated respiration of the microbial community could decrease over time because of
481 acclimation (Melillo et al. 1993; Todd-Brown et al., 2011). This mechanism shall be factored
482 into future soil decomposition analysis.

483 Except for model limitations mentioned above, additional uncertainties may come from
484 inadequate model parameterization and model assumptions. For example, a critical microbial
485 parameter, carbon use efficiency (CUE), is a primary control to soil CO₂ efflux. Higher CUE
486 indicates more microbial growth and more carbon uptake by plants, while lower CUE indicates
487 higher soil decomposition (Manzoni et al., 2012). Theoretical and empirical studies have
488 suggested that CUE depends on both temperature and substrate quality (Frey et al., 2013) and
489 decreases as temperature increases and nutrient availability decreases (Manzoni et al., 2012).
490 Our study considered the CUE sensitivity to temperature, but not nutrient availability. On the
491 other hand, some model assumptions can also cause uncertainties. For example, we assumed that
492 vegetation will not change during the transient simulation. However, over the past few decades
493 in northern high latitudes, temperature increases have led to vegetation shift from one type to
494 another (Hansen et al., 2006; White et al., 2000). The vegetation changes will affect carbon
495 cycling in these ecosystems.

496 While our analysis suggests it is important to incorporate microbial dormancy dynamics
497 into a process-based biogeochemistry model to more adequately simulate carbon dynamics in
498 northern high latitudes, we do confront modeling dilemmas. First, our process-based models
499 have a relatively large number of parameters, which unavoidably creates the “equifinality”
500 problem as recognized in our previous studies for the model (e.g., Tang and Zhuang, 2008,
501 2009). To alleviate this problem in this analysis, we have conducted parameter ensemble
502 simulations at both site and regional levels and presented our results with uncertainties, which
503 could be a standard approach for process-based complex biogeochemistry modeling analyses.
504 Second, incorporating more ecosystem processes increases the number of parameters in our
505 model, inducing even larger uncertainties for both site level and regional simulations. On the

506 one hand, the more complex model to a certain degree helps capture observations, on the other
507 hand, the model uncertainty has not been constrained or even enlarged. We highlight the need to
508 further investigate this trade-off within the modeling research community.

509

510 **5. Conclusions**

511 This study incorporated microbial dormancy into a detailed microbial-based soil
512 decomposition biogeochemistry model to examine the fate of large Arctic soil carbon under
513 changing climate conditions. Regional simulations using MIC-TEM-dormancy indicated that,
514 over the 20th century, the region is a carbon sink of 166.8 ± 97.7 Pg. This sink could decrease to
515 175.9 ± 105.4 Pg under the RCP 8.5 scenario or 125.4 ± 85.5 Pg under the RCP 2.6 scenario
516 during the 21st century. Whether considering microbial dormancy or not can cause large
517 differences in soil decomposition estimation between two models. Meanwhile, due to available
518 nitrogen affected by soil decomposition, net primary production is consequently influenced in
519 these two centuries. The combined changes in soil decomposition and net primary production led
520 to large differences in carbon budget estimation between two models. Compared with MIC-
521 TEM, MIC-TEM-dormancy projected 75.9 Pg more C stored in the terrestrial ecosystems over
522 the last century, 50.4 Pg and 125.2 Pg more C under the RCP 8.5 and RCP 2.6 scenarios,
523 respectively. This study highlights the importance of the representation of microbial dormancy in
524 earth system models in order to adequately quantify the carbon dynamics in northern high
525 latitudes.

526

527 **Acknowledgments**

528 This research was supported by a NSF project (IIS-1027955), a DOE project (DE-SC0008092),
529 and a NASA LCLUC project (NNX09AI26G) to Q. Z. We acknowledge the Rosen High
530 Performance Computing Center at Purdue for computing support. We thank the National Snow
531 and Ice Data center for providing Global Monthly EASE-Grid Snow Water Equivalent data,
532 National Oceanic and Atmospheric Administration for North American Regional Reanalysis
533 (NARR). We also acknowledge the World Climate Research Programme's Working Group on
534 Coupled Modeling Intercomparison Project CMIP5, and we thank the climate modeling groups
535 for producing and making available their model output. The data presented in this paper can be
536 accessed through our research website (<http://www.eaps.purdue.edu/ebdl/>)

537
538

539 **References:**

540 Allison, E. H., Perry, A. L., Badjeck, M.-C., Neil Adger, W., Brown, K., Conway, D., Halls, A.
541 S., Pilling, G. M., Reynolds, J. D., Andrew, N. L., and Dulvy, N. K.: Vulnerability of national
542 economies to the impacts of climate change on fisheries, *Fish and Fisheries*, 10, 173-196,
543 10.1111/j.1467-2979.2008.00310.x, 2009.

544 Allison, S. D., Wallenstein, M. D., and Bradford, M. A.: Soil-carbon response to warming
545 dependent on microbial physiology, *Nature Geoscience*, 3, 336-340, 10.1038/ngeo846, 2010.

546 Balser, T. C., Kinzig, A. P., and Firestone, M. K.: Linking soil microbial communities and
547 ecosystem functioning, *The functional consequences of biodiversity: Empirical progress and*
548 *theoretical extensions*, 265-293, 2002.

549 Blagodatskaya, E., and Kuzyakov, Y.: Active microorganisms in soil: Critical review of
550 estimation criteria and approaches, *Soil Biology and Biochemistry*, 67, 192-211,
551 10.1016/j.soilbio.2013.08.024, 2013.

552 Blagodatskaya, E., Khomyakov, N., Myachina, O., Bogomolova, I., Blagodatsky, S., and
553 Kuzyakov, Y.: Microbial interactions affect sources of priming induced by cellulose, *Soil*
554 *Biology and Biochemistry*, 74, 39-49, 10.1016/j.soilbio.2014.02.017, 2014.

555 Blagodatsky, S., Grote, R., Kiese, R., Werner, C., and Butterbach-Bahl, K.: Modelling of
556 microbial carbon and nitrogen turnover in soil with special emphasis on N-trace gases emission,
557 *Plant and soil*, 346, 297-330, 10.1007/s11104-011-0821-z, 2011.

558 Blagodatsky, S. A., Heinemeyer, O., and Richter, J.: Estimating the active and total soil
559 microbial biomass by kinetic respiration analysis, *Biol Fertil Soils*, 32, 73-81, 2000.

560 Bond-Lamberty, B., and Thomson, A.: Temperature-associated increases in the global soil
561 respiration record, *Nature*, 464, 579-582, 10.1038/nature08930, 2010.

562 Bond-Lamberty, B., Bailey, V. L., Chen, M., Gough, C. M., and Vargas, R.: Globally rising soil
563 heterotrophic respiration over recent decades, *Nature*, 560, 80-83, 10.1038/s41586-018-0358-x,
564 2018.

565 Bouskill, N. J., Tang, J., Riley, W. J., and Brodie, E. L.: Trait-based representation of biological
566 nitrification: model development, testing, and predicted community composition, *Frontiers in*
567 *microbiology*, 3, 364, 10.3389/fmicb.2012.00364, 2012.

568 Callaghan, T., Björn, L. O., Chernov, Y., Chapin, T., Christensen, T. R., Huntley, B., Ims, R.,
569 Jolly, D., Jonasson, S., Matveyeva, N., Panikov, N., Oechel, W., and Shaver, G.: Arctic tundra
570 and polar desert ecosystems, *Arctic climate impact assessment*, 243-352, 2005.

571 Carney, K. M., and Matson, P. A.: The influence of tropical plant diversity and composition on
572 soil microbial communities, *Microbial ecology*, 52, 226-238, 10.1007/s00248-006-9115-z, 2006.

573 Chmielewski, R. A. N., and Frank, J. F.: Formation of viable but nonculturable *Salmonella*
574 during starvation in chemically defined solutions, *Letters in Applied Microbiology*, 20, 380-384,
575 1995.

576 Classen, A. T., Sundqvist, M. K., Henning, J. A., Newman, G. S., Moore, J. A. M., Cregger, M.
577 A., Moorhead, L. C., and Patterson, C. M.: Direct and indirect effects of climate change on soil
578 microbial and soil microbial-plant interactions: What lies ahead?, *Ecosphere*, 6, art130,
579 10.1890/es15-00217.1, 2015.

580 Conant, R. T., Ryan, M. G., Ågren, G. I., Birge, H. E., Davidson, E. A., Eliasson, P. E., Evans, S.
581 E., Frey, S. D., Giardina, C. P., Hopkins, F. M., Hyvönen, R., Kirschbaum, M. U. F., Lavelle, J.
582 M., Leifeld, J., Parton, W. J., Megan Steinweg, J., Wallenstein, M. D., Martin Wetterstedt, J. Å.,
583 and Bradford, M. A.: Temperature and soil organic matter decomposition rates - synthesis of
584 current knowledge and a way forward, *Global change biology*, 17, 3392-3404, 10.1111/j.1365-
585 2486.2011.02496.x, 2011.

586 Coursolle, C., Margolis, H. A., Barr, A. G., Black, T. A., Amiro, B. D., McCaughey, J. H.,
587 Flanagan, L. B., Lafleur, P. M., Roulet, N. T., Bourque, C. P. A., Arain, M. A., Wofsy, S. C.,
588 Dunn, A., Morgenstern, K., Orchansky, A. L., Bernier, P. Y., Chen, J. M., Kidston, J., Saigusa,
589 N., and Hedstrom, N.: Late-summer carbon fluxes from Canadian forests and peatlands along an
590 east-west continental transect, *Canadian Journal of Forest Research*, 36, 783-800, 10.1139/x05-
591 270, 2006.

592 Davidson, E. A., Trumbore, S. E., and Amundson, R.: Biogeochemistry: soil warming and
593 organic carbon content, *Nature*, 408, 2000.

594 Davidson, E. A., and Janssens, I. A.: Temperature sensitivity of soil carbon decomposition and
595 feedbacks to climate change, *Nature*, 440, 165-173, 10.1038/nature04514, 2006.

596 Davidson, E. A., Janssens, I. A., and Luo, Y.: On the variability of respiration in terrestrial
597 ecosystems: moving beyond Q₁₀, *Global change biology*, 12, 154-164, 10.1111/j.1365-
598 2486.2005.01065.x, 2006.

599 Davidson, E. A., Samanta, S., Caramori, S. S., and Savage, K.: The Dual Arrhenius and
600 Michaelis-Menten kinetics model for decomposition of soil organic matter at hourly to seasonal
601 time scales, *Global change biology*, 18, 371-384, 10.1111/j.1365-2486.2011.02546.x, 2012.

602 Duan, Q., Sorooshian, S., and Gupta, V. K.: Optimal use of the SCE-UA global optimization
603 method for calibrating watershed models, *Journal of Hydrology*, 158, 265-284, 1994.

604 Evans, S. E., and Wallenstein, M. D.: Soil microbial community response to drying and
605 rewetting stress: does historical precipitation regime matter?, *Biogeochemistry*, 109, 101-116,
606 10.1007/s10533-011-9638-3, 2011.

607 Fierer, N., Morse, J. L., Berthrong, S. T., Bernhardt, E. S., and Jackson, R. B.: Environmental
608 controls on the landscape - scale biogeography of stream bacterial communities, *Ecology*, 88,
609 2162-2173, 2007.

610 Frey, S. D., Lee, J., Melillo, J. M., and Six, J.: The temperature response of soil microbial
611 efficiency and its feedback to climate, *Nature Climate Change*, 3, 395-398,
612 10.1038/nclimate1796, 2013.

613 German, D. P., Marcelo, K. R. B., Stone, M. M., and Allison, S. D.: The Michaelis-Menten
614 kinetics of soil extracellular enzymes in response to temperature: a cross-latitudinal study,
615 *Global change biology*, 18, 1468-1479, 10.1111/j.1365-2486.2011.02615.x, 2012.

616 Gilmanov, T. G., Tieszen, L. L., Wylie, B. K., Flanagan, L. B., Frank, A. B., Haferkamp, M. R.,
617 Meyers, T. P., and Morgan, J. A.: Integration of CO₂ flux and remotely-sensed data for primary
618 production and ecosystem respiration analyses in the Northern Great Plains: potential for
619 quantitative spatial extrapolation, *Global Ecology and Biogeography*, 14, 271-292,
620 10.1111/j.1466-822X.2005.00151.x, 2005.

621 Gough, C. M., Hardiman, B. S., Nave, L. E., Bohrer, G., Maurer, K. D., Vogel, C. S.,
622 Nadelhoffer, K. J., and Curtis, P. S.: Sustained carbon uptake and storage following moderate
623 disturbance in a Great Lakes forest, *Ecological Applications*, 23, 1202-1215, 2013.

624 Goulden, M. L., Winston, G. C., McMillan, A. M. S., Litvak, M. E., Read, E. L., Rocha, A. V.,
625 and Rob Elliot, J.: An eddy covariance mesonet to measure the effect of forest age on
626 land-atmosphere exchange, *Global change biology*, 12, 2146-2162, 10.1111/j.1365-
627 2486.2006.01251.x, 2006.

628 Graham, E. B., Wieder, W. R., Leff, J. W., Weintraub, S. R., Townsend, A. R., Cleveland, C. C.,
629 Philippot, L., and Nemergut, D. R.: Do we need to understand microbial communities to predict
630 ecosystem function? A comparison of statistical models of nitrogen cycling processes, *Soil
631 Biology and Biochemistry*, 68, 279-282, 10.1016/j.soilbio.2013.08.023, 2014.

632 Graham, E. B., Knelman, J. E., Schindlbacher, A., Siciliano, S., Breulmann, M., Yannarell, A.,
633 Beman, J. M., Abell, G., Philippot, L., Prosser, J., Foulquier, A., Yuste, J. C., Glanville, H. C.,
634 Jones, D. L., Angel, R., Salminen, J., Newton, R. J., Burgmann, H., Ingram, L. J., Hamer, U.,
635 Siljanen, H. M., Peltoniemi, K., Potthast, K., Banerjee, L., Hartmann, M., Banerjee, S., Yu, R. Q.,
636 Nogaro, G., Richter, A., Koranda, M., Castle, S. C., Goberna, M., Song, B., Chatterjee, A.,
637 Nunes, O. C., Lopes, A. R., Cao, Y., Kaisermann, A., Hallin, S., Strickland, M. S., Garcia-
638 Pausas, J., Barba, J., Kang, H., Isobe, K., Papaspyrou, S., Pastorelli, R., Lagomarsino, A.,
639 Lindstrom, E. S., Basiliko, N., and Nemergut, D. R.: Microbes as Engines of Ecosystem
640 Function: When Does Community Structure Enhance Predictions of Ecosystem Processes?,
641 *Frontiers in microbiology*, 7, 214, 10.3389/fmicb.2016.00214, 2016.

642 Griffis, T. J., Lee, X., Baker, J. M., Billmark, K., Schultz, N., Erickson, M., Zhang, X.,
643 Fassbinder, J., Xiao, W., and Hu, N.: Oxygen isotope composition of evapotranspiration and its
644 relation to C₄ photosynthetic discrimination, *Journal of Geophysical Research*, 116,
645 10.1029/2010jg001514, 2011.

646 Hagerty, S. B., van Groenigen, K. J., Allison, S. D., Hungate, B. A., Schwartz, E., Koch, G. W.,
647 Kolka, R. K., and Dijkstra, P.: Accelerated microbial turnover but constant growth efficiency
648 with warming in soil, *Nature Climate Change*, 4, 903-906, 10.1038/nclimate2361, 2014.

649 Hansen, J., Sato, M., Ruedy, R., Lo, K., Lea, D. W., and Medina-Elizade, M.: Global
650 temperature change, *Proceedings of the National Academy of Sciences of the United States of
651 America*, 103, 14288-14293, 10.1073/pnas.0606291103, 2006.

652 Harder, w., and Dijkhuizen, L.: Physiological responses to nutrient limitation, *Annual Review of
653 Microbiology*, 37, 1983.

654 Harris, I., Jones, P. D., Osborn, T. J., and Lister, D. H.: Updated high-resolution grids of monthly
655 climatic observations - the CRU TS3.10 Dataset, *International Journal of Climatology*, 34, 623-
656 642, 10.1002/joc.3711, 2014.

657 He, Y., Yang, J., Zhuang, Q., Harden, J. W., McGuire, A. D., Liu, Y., Wang, G., and Gu, L.:
658 Incorporating microbial dormancy dynamics into soil decomposition models to improve
659 quantification of soil carbon dynamics of northern temperate forests, *Journal of Geophysical
660 Research: Biogeosciences*, 120, 2596-2611, 10.1002/2015jg003130, 2015.

661 Hiller, R. V., McFadden, J. P., and Kljun, N.: Interpreting CO₂ Fluxes Over a Suburban Lawn:
662 The Influence of Traffic Emissions, *Boundary-Layer Meteorology*, 138, 215-230,
663 10.1007/s10546-010-9558-0, 2010.

664 Houghton, R. A.: Balancing the Global Carbon Budget, *Annual Review of Earth and Planetary
665 Sciences*, 35, 313-347, 10.1146/annurev.earth.35.031306.140057, 2007.

666 Hugelius, G., Strauss, J., Zubrzycki, S., Harden, J. W., Schuur, E. A. G., Ping, C. L.,
667 Schirmer, L., Grosse, G., Michaelson, G. J., Koven, C. D., and others, Donnell, J. A.,
668 Elberling, B., Mishra, U., Camill, P., Yu, Z., Palmtag, J., and Kuhry, P.: Estimated stocks of
669 circumpolar permafrost carbon with quantified uncertainty ranges and identified data gaps,
670 *Biogeosciences*, 11, 6573-6593, 10.5194/bg-11-6573-2014, 2014.

671 Jenkins, J. P., Richardson, A. D., Braswell, B. H., Ollinger, S. V., Hollinger, D. Y., and Smith,
672 M. L.: Refining light-use efficiency calculations for a deciduous forest canopy using
673 simultaneous tower-based carbon flux and radiometric measurements, *Agricultural and Forest
674 Meteorology*, 143, 64-79, 10.1016/j.agrformet.2006.11.008, 2007.

675 Kaiser, C., Franklin, O., Dieckmann, U., and Richter, A.: Microbial community dynamics
676 alleviate stoichiometric constraints during litter decay, *Ecology letters*, 17, 680-690,
677 10.1111/ele.12269, 2014.

678 Knorr, W., Prentice, I. C., House, J. I., and Holland, E. A.: Long-term sensitivity of soil carbon
679 turnover to warming, *Nature*, 433, 2005.

680 Lawrence, C. R., Neff, J. C., and Schimel, J. P.: Does adding microbial mechanisms of
681 decomposition improve soil organic matter models? A comparison of four models using data
682 from a pulsed rewetting experiment, *Soil Biology and Biochemistry*, 41, 1923-1934,
683 10.1016/j.soilbio.2009.06.016, 2009.

684 Lennon, J. T., and Jones, S. E.: Microbial seed banks: the ecological and evolutionary
685 implications of dormancy, *Nature reviews. Microbiology*, 9, 119-130, 10.1038/nrmicro2504,
686 2011.

687 Lloyd, A. H., Rupp, T. S., Fastie, C. L., and Starfield, A. M.: Patterns and dynamics of treeline
688 advance on the Seward Peninsula, Alaska, *Journal of Geophysical Research*, 108,
689 10.1029/2001jd000852, 2002.

690 Manzoni, S., Taylor, P., Richter, A., Porporato, A., and Agren, G. I.: Environmental and
691 stoichiometric controls on microbial carbon-use efficiency in soils, *The New phytologist*, 196,
692 79-91, 10.1111/j.1469-8137.2012.04225.x, 2012.

693 McEwing, K. R., Fisher, J. P., and Zona, D.: Environmental and vegetation controls on the
694 spatial variability of CH₄ emission from wet-sedge and tussock tundra ecosystems in the Arctic,
695 *Plant and soil*, 388, 37-52, 10.1007/s11104-014-2377-1, 2015.

696 McGuire, A. D., Melillo, J. M., Joyce, L. A., Kicklighter, D. W., Grace, A. L., III, B. M., and
697 Vorosmarty, C. J.: Interactions between carbon and nitrogen dynamics in estimating net primary
698 productivity for potential vegetation in North America, *Global Biogeochemical Cycles*, 6, 101-
699 124, 1992.

700 McGuire, A. D., Melillo, J. M., Kicklighter, D. W., and Joyce, L. A.: Equilibrium responses of
701 soil carbon to climate change: Empirical and process-based estimates, *Journal of Biogeography*,
702 22, 785-796, 1995.

703 McGuire, A. D., and Hobbie, J. E.: Global climate change and the equilibrium responses of
704 carbon storage in arctic and subarctic regions, In *Modeling the Arctic system: A workshop report*
705 on the state of modeling in the Arctic System Science program, 53-54, 1997.

706 McGuire, A. D., Anderson, L. G., Christensen, T. R., Dallimore, S., Guo, L., Hayes, D. J.,
707 Heimann, M., Lorenson, T. D., Macdonald, R. W., and Roulet, N.: Sensitivity of the carbon
708 cycle in the Arctic to climate change, *Ecological Monographs*, 79, 523-555, 2009.

709 McGuire, K. L., and Treseder, K. K.: Microbial communities and their relevance for ecosystem
710 models: Decomposition as a case study, *Soil Biology and Biochemistry*, 42, 529-535,
711 10.1016/j.soilbio.2009.11.016, 2010.

712 Me´tris, A., Gerrard, A. M., Cumming, R. H., Weigner, P., and Paca, J.: Modelling shock
713 loadings and starvation in the biofiltration of toluene and xylene, *Journal of Chemical*
714 *Technology and Biotechnology*, 76, 565-572, 2001.

715 Melillo, J. M., McGuire, A. D., Kicklighter, D. W., III, B. M., Vorosmarty, C. J., and Schloss, A.
716 L.: Global climate change and terrestrial net primary production, *Nature*, 363, 1993.

717 Melillo, J. M., Butler, S., Johnson, J., Mohan, J., Steudler, P., Lux, H., Burrows, E., Bowles, F.,
718 Smith, R., Scott, L., Vario, C., Hill, T., Burton, A., Zhou, Y.-M., and Tang, J.: Soil warming,
719 carbon - nitrogen interactions, and forest carbon budgets, *PNAS*, 108, 9508-9512, 2011.

720 Merbold, L., Kutsch, W. L., Corradi, C., Kolle, O., Rebmann, C., Stoy, P. C., Zimov, S. A., and
721 Schulze, E. D.: Artificial drainage and associated carbon fluxes (CO₂/CH₄) in a tundra
722 ecosystem, *Global change biology*, 15, 2599-2614, 10.1111/j.1365-2486.2009.01962.x, 2009.

723 Moorhead, D. L., and Sinsabaugh, R. L.: A theoretical model of litter decay and microbial
724 interaction, *Ecological Monographs*, 76, 151-174, 2006.

725 Oechel, W. C., Laskowski, C. A., Burba, G., Gioli, B., and Kalhori, A. A. M.: Annual patterns
726 and budget of CO₂ flux in an Arctic tussock tundra ecosystem, *Journal of Geophysical Research:*
727 *Biogeosciences*, 119, 323-339, 10.1002/2013jg002431, 2014.

728 P.J. Hanson, N. T. E., C.T. Garten, J.A. Andrews: Separating root and soil microbial
729 contributions to soil respiration: A review of methods and observations, *Biogeochemistry*, 48,
730 115-146, 2000.

731 Parton, W. J., Scurlock, J. M. O., Ojima, D. S., Gilmanov, T. G., Scholes, R. J., Schimel, D. S.,
732 Kirchner, T., Menaut, J. C., Seastedt, T., Moya, E. G., Kamnalrut, A., and Kinyamario, J. I.:
733 Observations and modeling of biomass and soil organic matter dynamics for the grassland biome
734 worldwide, *Global Biogeochemical Cycles*, 7, 785-809, 1993.

735 Raich, J. W., Rastetter, E. B., Melillo, J. M., Kicklighter, D. W., Steudler, P. A., Peterson, B. J.,
736 Grace, A. L., III, B. M., and Vorosmarty, C. J.: Potential net primary productivity in South
737 America: application of a global model, *Ecological Applications*, 1, 399-429, 1991.

738 Richardson, A. D., Jenkins, J. P., Braswell, B. H., Hollinger, D. Y., Ollinger, S. V., and Smith,
739 M. L.: Use of digital webcam images to track spring green-up in a deciduous broadleaf forest,
740 *Oecologia*, 152, 323-334, 10.1007/s00442-006-0657-z, 2007.

741 Running, S. W., and Coughlan, J. C.: A general model of forest ecosystem processes for regional
742 applications I. Hydrologic balance, canopy gas exchange and primary production processes.,
743 *Ecological Modelling*, 42, 125-154, 1988.

744 Schimel, D. S.: Terrestrial ecosystems and the carbon cycle, *Global change biology*, 1, 77-91,
745 1995.

746 Schimel, D. S., House, J. I., Hibbard, K. A., Bousquet, P., Ciais, P., Peylin, P., Braswell, B. H.,
747 Apps, M. J., Baker, D., Bondeau, A., Canadell, J., Churkina, G., Cramer, W., Denning, A. S.,
748 Field, C. B., Friedlingstein, P., Goodale, C., Heimann, M., Houghton, R. A., Melillo, J. M., III,
749 B. M., Murdiyarso, D., Noble, I., Pacala, S. W., Prentice, I. C., Raupach, M. R., Rayner, P. J.,
750 Scholes, R. J., Steffen, W. L., and Wirth, C.: Recent patterns and mechanisms of carbon
751 exchange by terrestrial ecosystems, *Nature*, 414, 2001.

752 Schimel, J.: Microbes and global carbon, *Nature Climate Change*, 3, 867-868,
753 10.1038/nclimate2015, 2013.

754 Schimel, J. P., and Weintraub, M. N.: The implications of exoenzyme activity on microbial
755 carbon and nitrogen limitation in soil: a theoretical model, *Soil Biology and Biochemistry*, 35,
756 549-563, 10.1016/s0038-0717(03)00015-4, 2003.

757 Schimel, J. P., and Schaeffer, S. M.: Microbial control over carbon cycling in soil, *Frontiers in*
758 *microbiology*, 3, 348, 10.3389/fmicb.2012.00348, 2012.

759 Schlesinger, W. H., and Andrews, J. A.: Soil respiration and the global carbon cycle,
760 *Biogeochemistry*, 48, 7-20, 2000.

761 Schmidt, M. W., Torn, M. S., Abiven, S., Dittmar, T., Guggenberger, G., Janssens, I. A., Kleber,
762 M., Kogel-Knabner, I., Lehmann, J., Manning, D. A., Nannipieri, P., Rasse, D. P., Weiner, S.,
763 and Trumbore, S. E.: Persistence of soil organic matter as an ecosystem property, *Nature*, 478,
764 49-56, 10.1038/nature10386, 2011.

765 Serreze, M. C., and Francis, J. A.: The Arctic on the fast track of change, *Weather*, 61, 65-69,
766 2006.

767 Stolpovsky, K., Martinez-Lavanchy, P., Heipieper, H. J., Van Cappellen, P., and Thullner, M.:
768 Incorporating dormancy in dynamic microbial community models, *Ecological Modelling*, 222,
769 3092-3102, 10.1016/j.ecolmodel.2011.07.006, 2011.

770 Stow, D. A., Hope, A., McGuire, D., Verbyla, D., Gamon, J., Huemmrich, F., Houston, S.,
771 Racine, C., Sturm, M., Tape, K., Hinzman, L., Yoshikawa, K., Tweedie, C., Noyle, B.,
772 Silapaswan, C., Douglas, D., Griffith, B., Jia, G., Epstein, H., Walker, D., Daeschner, S.,
773 Petersen, A., Zhou, L., and Myneni, R.: Remote sensing of vegetation and land-cover change in
774 Arctic Tundra Ecosystems, *Remote Sensing of Environment*, 89, 281-308,
775 10.1016/j.rse.2003.10.018, 2004.

776 Strickland, M. S., Lauber, C., Fierer, N., and Bradford, M. A.: Testing the functional
777 significance of microbial community composition, *Ecology*, 90, 441-451, 2009.

778 Tang, J., Q. Zhuang (2009) A global sensitivity analysis and Bayesian inference framework for
779 improving the parameter estimation and prediction of a process-based Terrestrial Ecosystem
780 Model *J. Geophys. Res.*, 114, D15303, doi:10.1029/2009JD011724., 2009.

781 Tang, J., Q. Zhuang (2008) Equifinality in parameterization of process-based biogeochemistry
782 models: A significant uncertainty source to the estimation of regional carbon dynamics *J.*
783 *Geophys. Res.*, 113, G04010, doi:10.1029/2008JG000757, 2008.

784 Tang, J., and Riley, W. J.: Weaker soil carbon–climate feedbacks resulting from microbial and
785 abiotic interactions, *Nature Climate Change*, 5, 56-60, 10.1038/nclimate2438, 2014.

786 Tape, K. E. N., Sturm, M., and Racine, C.: The evidence for shrub expansion in Northern Alaska
787 and the Pan-Arctic, *Global change biology*, 12, 686-702, 10.1111/j.1365-2486.2006.01128.x,
788 2006.

789 Tarnocai, C., Canadell, J. G., Schuur, E. A. G., Kuhry, P., Mazhitova, G., and Zimov, S.: Soil
790 organic carbon pools in the northern circumpolar permafrost region, *Global Biogeochemical*
791 *Cycles*, 23, n/a-n/a, 10.1029/2008gb003327, 2009.

792 Thullner, M., Van Cappellen, P., and Regnier, P.: Modeling the impact of microbial activity on
793 redox dynamics in porous media, *Geochimica et Cosmochimica Acta*, 69, 5005-5019,
794 10.1016/j.gca.2005.04.026, 2005.

795 Todd-Brown, K. E. O., Hopkins, F. M., Kivlin, S. N., Talbot, J. M., and Allison, S. D.: A
796 framework for representing microbial decomposition in coupled climate models,
797 *Biogeochemistry*, 109, 19-33, 10.1007/s10533-011-9635-6, 2011.

798 Todd-Brown, K. E. O., Randerson, J. T., Post, W. M., Hoffman, F. M., Tarnocai, C., Schuur, E.
799 A. G., and Allison, S. D.: Causes of variation in soil carbon simulations from CMIP5 Earth
800 system models and comparison with observations, *Biogeosciences*, 10, 1717-1736, 10.5194/bg-
801 10-1717-2013, 2013.

802 Treseder, K. K., Balsler, T. C., Bradford, M. A., Brodie, E. L., Dubinsky, E. A., Eviner, V. T.,
803 Hofmockel, K. S., Lennon, J. T., Levine, U. Y., MacGregor, B. J., Pett-Ridge, J., and Waldrop,
804 M. P.: Integrating microbial ecology into ecosystem models: challenges and priorities,
805 *Biogeochemistry*, 109, 7-18, 10.1007/s10533-011-9636-5, 2011.

806 W. D. Billings, K. M. P., G. R. Shaver, A. W. Trent: Root Growth, Respiration, and Carbon
807 Dioxide Evolution in an Arctic Tundra Soil, *Arctic and Alpine Research*, 9, 129-137,
808 10.1080/00040851.1977.12003908, 1977.

809 Wang, G., M. A. M., Lianhong Gu, Christopher W. Schadt: Representation of Dormant and
810 Active Microbial Dynamics for Ecosystem Modeling, *Public Library of Science*, 9,
811 10.1371/journal.pone.0089252.g001, 2014.

812 Wang, G., Jagadamma, S., Mayes, M. A., Schadt, C. W., Steinweg, J. M., Gu, L., and Post, W.
813 M.: Microbial dormancy improves development and experimental validation of ecosystem
814 model, *The ISME journal*, 9, 226-237, 10.1038/ismej.2014.120, 2015.

815 Wang Wei, F. J., T. Oikawa: Contribution of Root and Microbial Respiration to Soil CO₂ Efflux
816 and Their Environmental Controls in a Humid Temperate Grassland of Japan, *Pedosphere*, 19,
817 31-39, 2009.

818 Werf, H. V. d., and Verstraete, W.: Estimation of active soil microbial biomass by mathematical
819 analysis of respiration curves: relation to conventional estimation of total biomass, *Soil Biology*
820 *and Biochemistry*, 19, 267-271, 1987.

821 White, A., Cannell, M. G. R., and Friend, A. D.: The high-latitude terrestrial carbon sink: a
822 model analysis *Global change biology*, 6, 227-245, 2000.

823 Wieder, W. R., Bonan, G. B., and Allison, S. D.: Global soil carbon projections are improved by
824 modelling microbial processes, *Nature Climate Change*, 3, 909-912, 10.1038/nclimate1951,
825 2013.

826 Xu, X., Schimel, J. P., Thornton, P. E., Song, X., Yuan, F., and Goswami, S.: Substrate and
827 environmental controls on microbial assimilation of soil organic carbon: a framework for Earth
828 system models, *Ecology letters*, 17, 547-555, 10.1111/ele.12254, 2014.

829 Zha, J., and Zhuang, Q.: Microbial decomposition processes and vulnerable arctic soil organic
830 carbon in the 21st century, *Biogeosciences*, 15, 5621-5634, 10.5194/bg-15-5621-2018, 2018a.

831 Zha, J., and Zhuang, Q.: Microbial decomposition processes and vulnerable Arctic soil organic
832 carbon in the 21st century, *Biogeosciences Discussions*, 1-34, 10.5194/bg-2018-241, 2018b.

833 Zhou, L., Tucker, C. J., Kaufmann, R. K., Slayback, D., Shabanov, N. V., and Myneni, R. B.:
834 Variations in northern vegetation activity inferred from satellite data of vegetation index during
835 1981 to 1999, *Journal of Geophysical Research: Atmospheres*, 106, 20069-20083,
836 10.1029/2000jd000115, 2001.

837 Zhuang, Q., Romanovsky, V. E., and McGuire, A. D.: Incorporation of a permafrost model into a
838 large-scale ecosystem model: Evaluation of temporal and spatial scaling issues in simulating soil
839 thermal dynamics, *Journal of Geophysical Research: Atmospheres*, 106, 33649-33670,
840 10.1029/2001jd900151, 2001.

841 Zhuang, Q., McGuire, A. D., O'Neill, K. P., Harden, J. W., Romanovsky, V. E., and Yarie, J.:
842 Modeling soil thermal and carbon dynamics of a fire chronosequence in interior Alaska, *Journal*
843 *of Geophysical Research*, 108, 10.1029/2001jd001244, 2002.

844 Zhuang, Q., He, J., Lu, Y., Ji, L., Xiao, J., and Luo, T.: Carbon dynamics of terrestrial
845 ecosystems on the Tibetan Plateau during the 20th century: an analysis with a process-based
846 biogeochemical model, *Global Ecology and Biogeography*, 19, 649-662, 10.1111/j.1466-
847 8238.2010.00559.x, 2010.

848 Zhuang, Q., Zhu, X., He, Y., Prigent, C., Melillo, J. M., David McGuire, A., Prinn, R. G., and
849 Kicklighter, D. W.: Influence of changes in wetland inundation extent on net fluxes of carbon
850 dioxide and methane in northern high latitudes from 1993 to 2004, *Environmental Research*
851 *Letters*, 10, 095009, 10.1088/1748-9326/10/9/095009, 2015.

852 Zhuang, Q., McGuire, A. D., Melillo, J. M., Klein, J. S., Dargaville, R. J., Kicklighter, D. W.,
853 Myneni, R. B., Dong, J., Romanovsky, V. E., Harden, J., and Hobbie, J. E.: Carbon cycling in
854 extratropical terrestrial ecosystems of the Northern Hemisphere during the 20th century: a
855 modeling analysis of the influences of soil thermal dynamics, *Tellus B: Chemical and Physical*
856 *Meteorology*, 55, 751-776, 10.3402/tellusb.v55i3.16368, 2016.

857
858
859
860

861

862 **Author contributions.** Q.Z. designed the study. J.Z. conducted model development, simulation
863 and analysis. J.Z. and Q. Z. wrote the paper.

864 **Competing financial interests.** The submission has no competing financial interests.

865 **Materials & Correspondence.** Correspondence and material requests should be addressed to
866 qzhuang@purdue.edu.

867

868

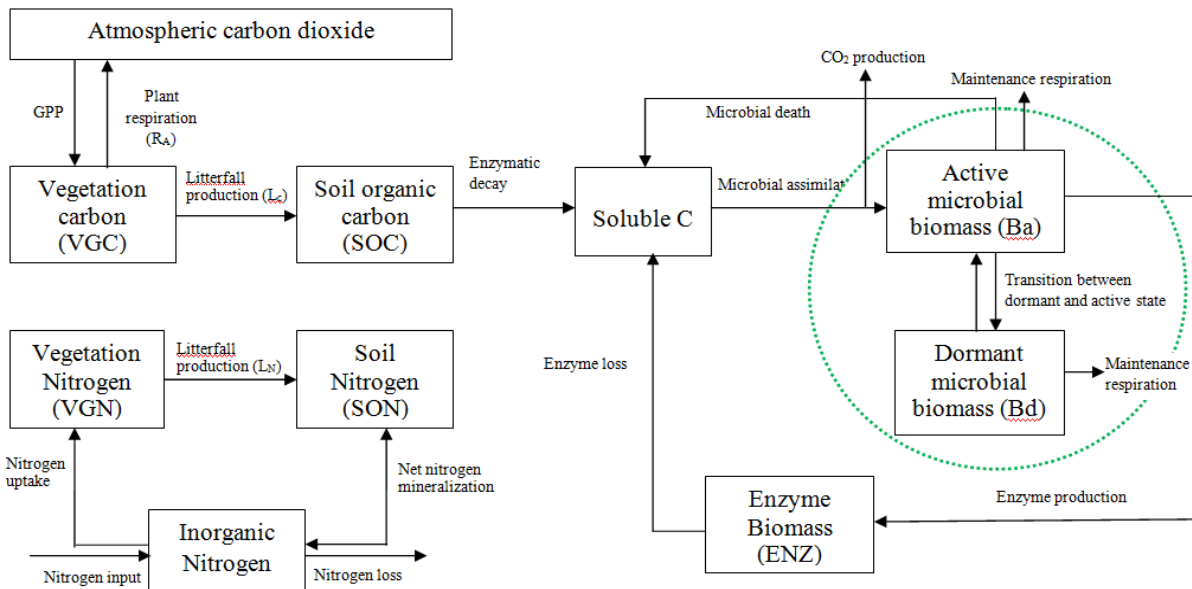
869

870

871

872

873



874

875

876

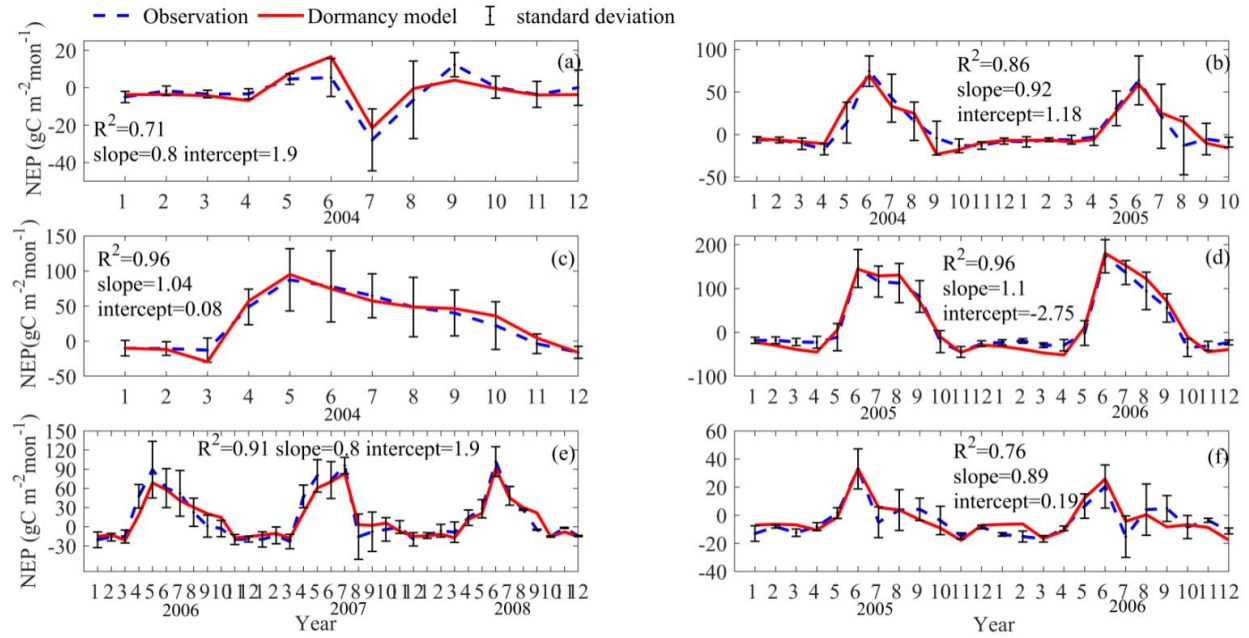
877

878

879

880

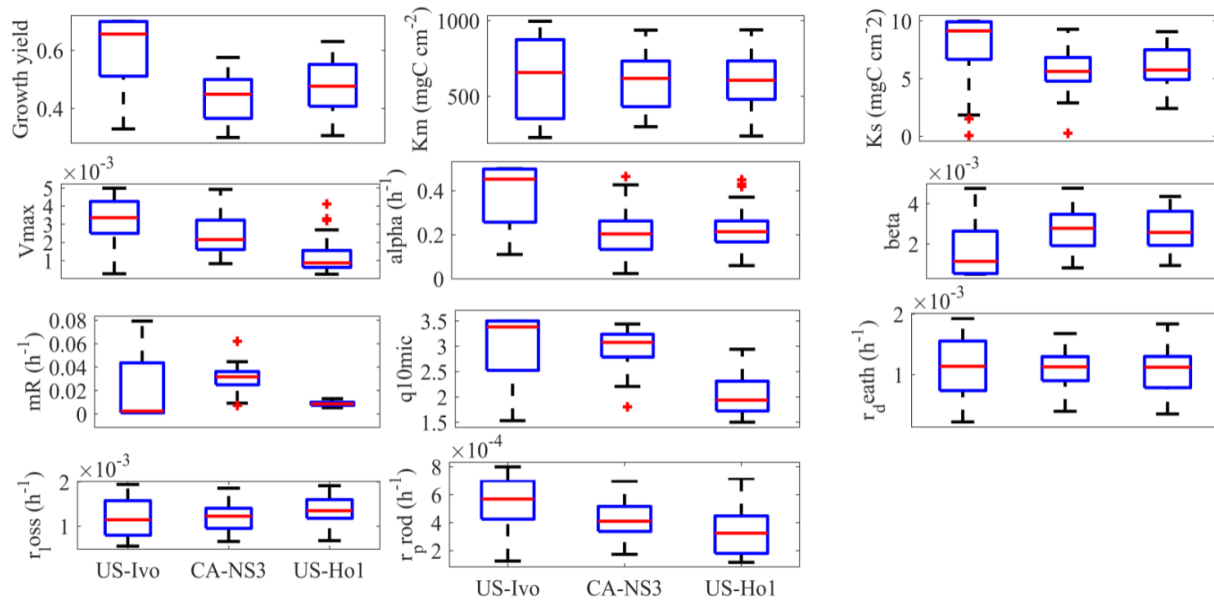
Figure 1. Framework of the dormancy model: microbial biomass is split into two parts, active microbial biomass and dormant microbial biomass (shown in the green dashed circle). Maintenance respiration from these two parts, and the CO₂ production through microbial assimilation contributes to heterotrophic respiration. The model was revised based on Zha & Zhuang (2018).



881
882
883
884
885
886
887
888

Figure 2. Comparison between observed and simulated NEP ($\text{gC m}^{-2}\text{mon}^{-1}$) at: (a) Ivotuk (alpine tundra), (b) UCI-1964 burn site (boreal forest), (c) Howland Forest (main tower) (temperate coniferous forest), (d) Univ. of Mich. Biological Station (Temperate deciduous forest), (e) KUOM Turfgrass Field (Grassland), and (f) Atqasuk (Wet tundra). Note: scales are different. Error bars represent standard errors among daily measure data in one month.

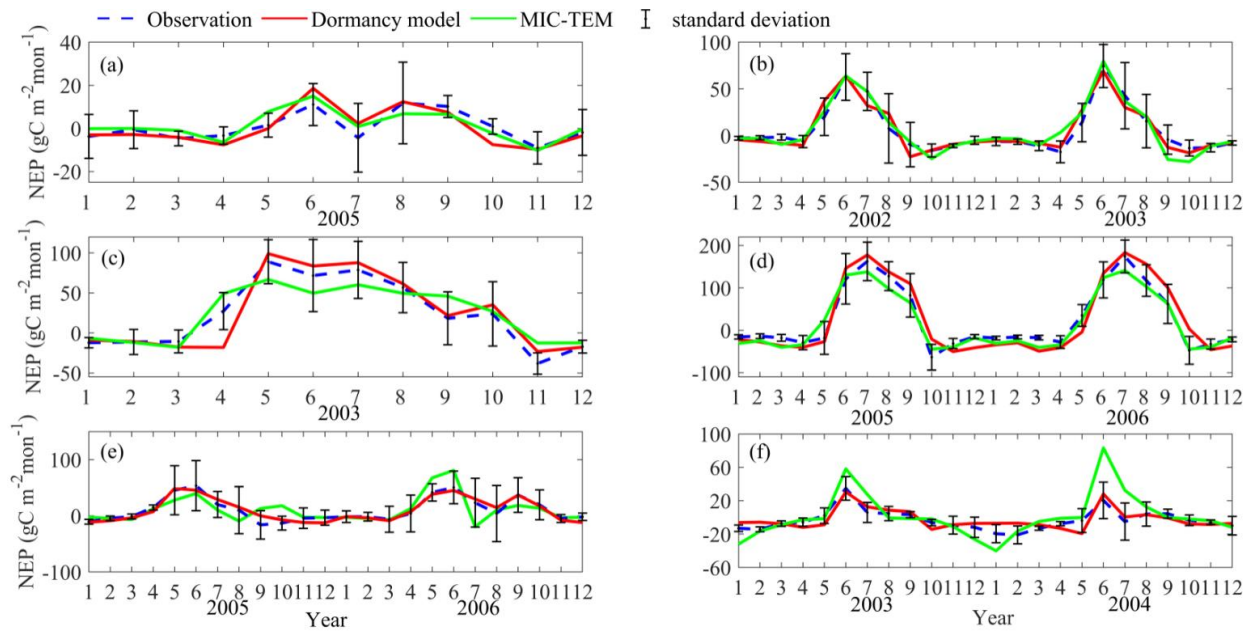
889



890

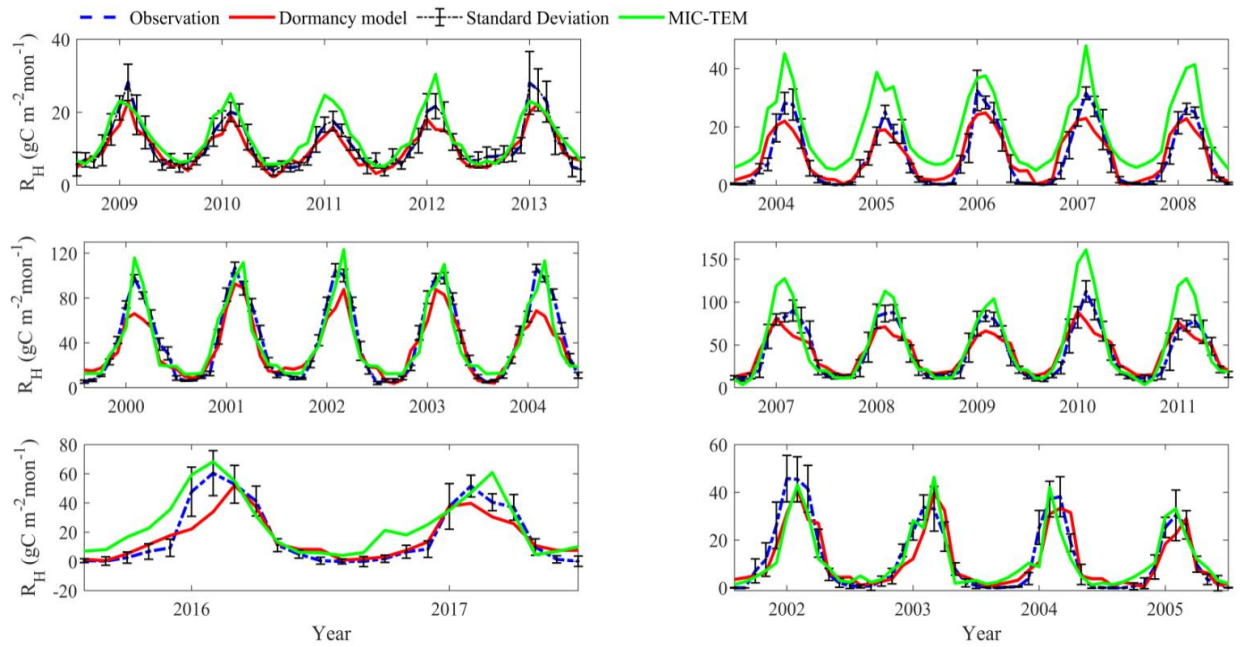
891

892 Figure 3. Boxplot of parameter posterior distribution that are obtained after ensemble inverse
893 modeling for MIC-TEM-dormancy all six sites: US-Ivo: Iivotuk (alpine tundra), CA-NS3: UCI-
894 1964 burn site (boreal forest), US-Ho1: Howland Forest (temperate coniferous forest), US-UMB:
895 Univ. of Mich. Biological Station (temperate deciduous forest), US-KUT: KUOM Turfgrass
896 Field (grassland), US-Atq: Atqasuk (wet tundra).
897



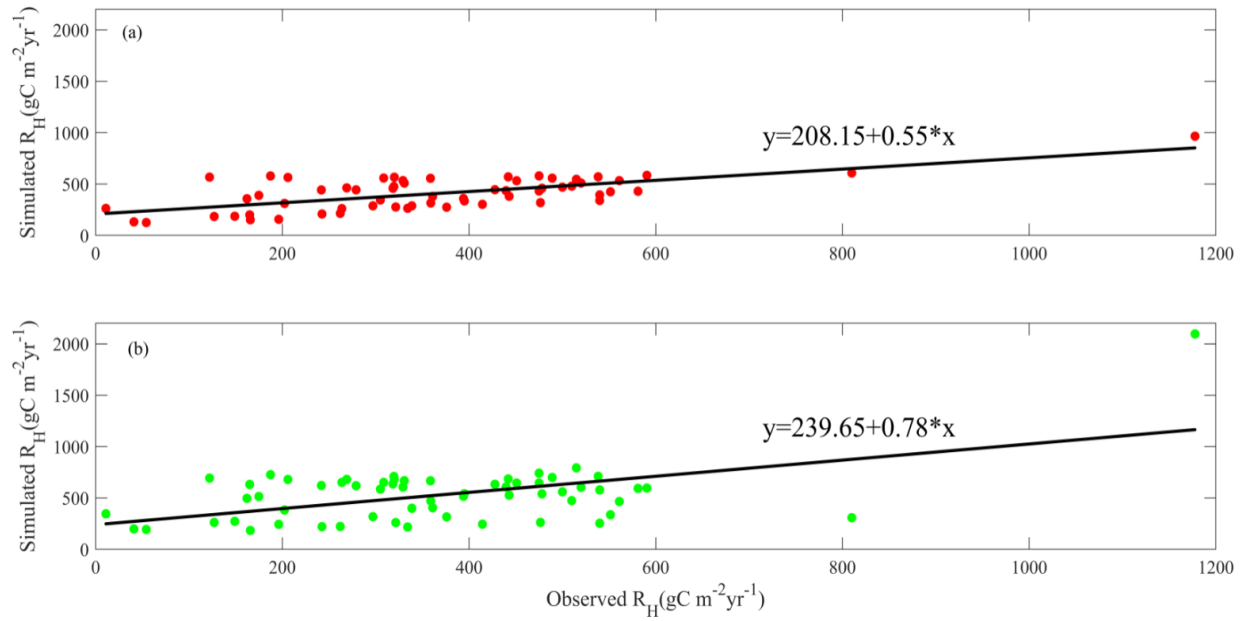
898
899

900 Figure 4. Comparison between observed and simulated NEP ($\text{gC m}^{-2}\text{mon}^{-1}$) at: (a) Ivotuk (alpine
901 tundra), (b) UCI-1964 burn site (boreal forest), (c) Howland Forest (main tower) (temperate
902 coniferous forest), (d) Bartlett Experimental Forest (Temperate deciduous forest), (e) Brookings
903 (Grassland), and (f) Atqasuk (Wet tundra). Note: scales are different.
904



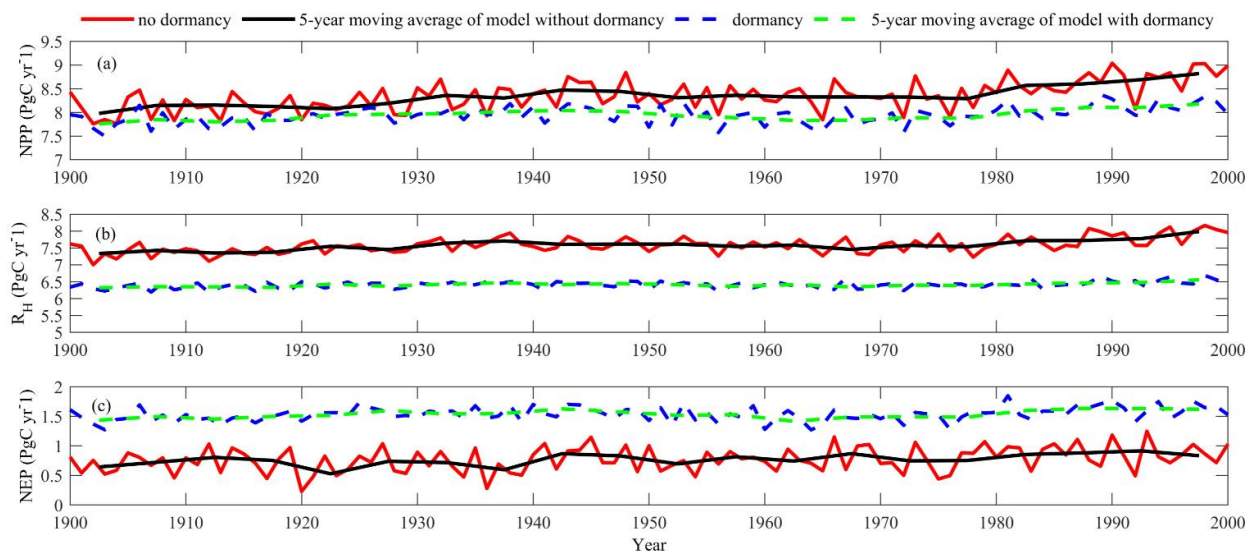
905
 906
 907
 908
 909
 910
 911
 912
 913
 914
 915
 916
 917
 918
 919

Figure 5. Comparison between observed and simulated R_H ($\text{gC m}^{-2} \text{mon}^{-1}$) at: (a) US-EML (alpine tundra), (b) CA-SJ2 (boreal forest), (c) US-Ho2 (temperate coniferous forest), (d) US-UMB (Temperate deciduous forest), (e) US-Ro4 (Grassland), and (f) RU-Che (Wet tundra). Note: scales are different.



920
 921
 922
 923
 924
 925
 926
 927
 928
 929
 930

Figure 6. Linear regression between simulated and observed annual R_H (gC m⁻² yr⁻¹) for: (a) MIC-TEM-dormancy, and (b) MIC-TEM.



931

932 Figure 7. Simulated annual net primary production (NPP, top panel), heterotrophic respiration (R_H ,
 933 center panel) and net ecosystem production (NEP, bottom panel) during the 20th century by
 934 dormancy model and MIC-TEM, respectively.

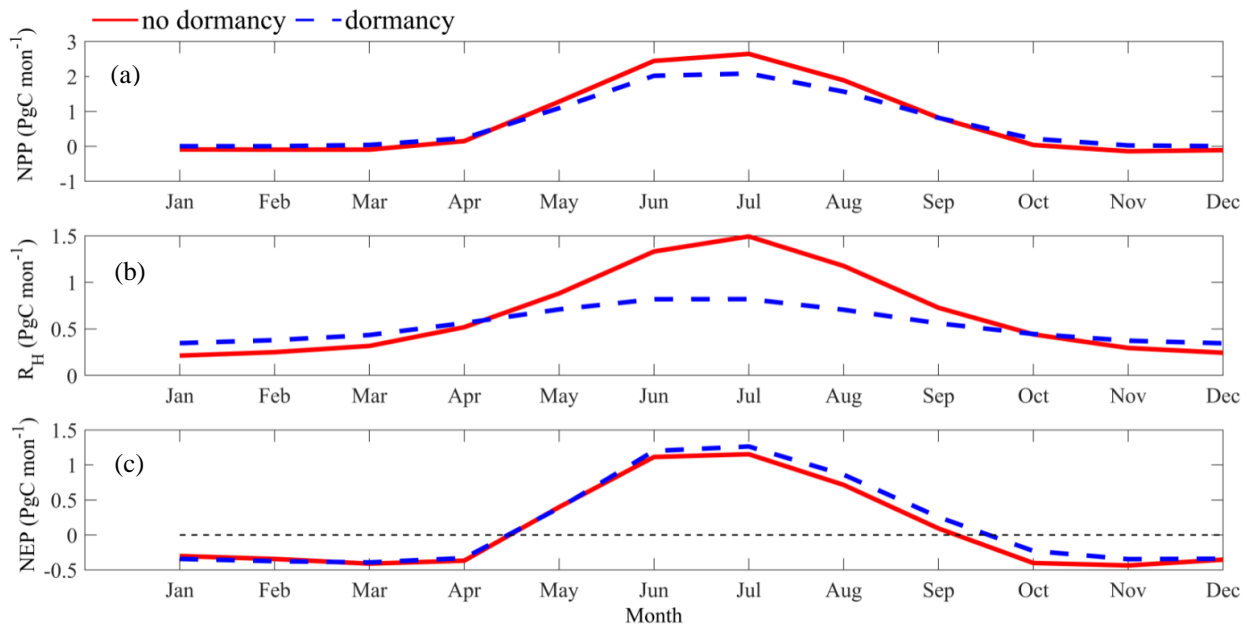
935

936

937

938

939



940

941 Figure 8. Regional annual seasonal pattern of simulated (a) net primary production (NPP, top
 942 panel), (b) heterotrophic respiration (R_H , center panel) and (c) net ecosystem production (NEP,
 943 bottom panel) during the 1990s from dormancy model and MIC-TEM. The region is all land
 944 areas north of 45 °N.

945

946

947

948

949

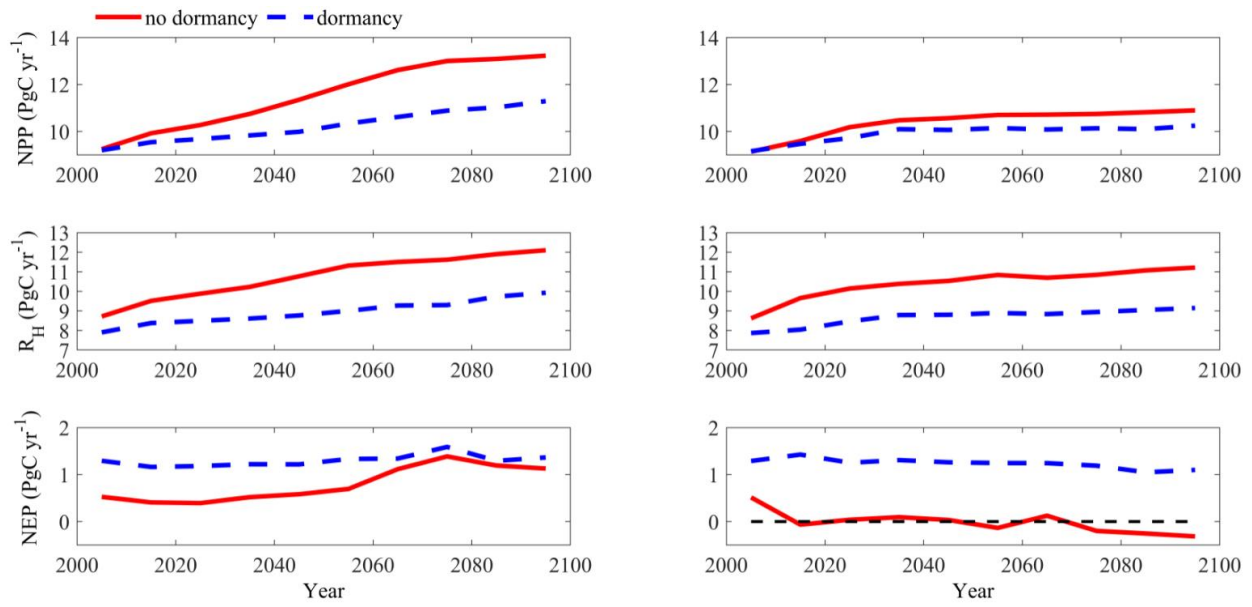
950

951

952

953

954



955

956 Figure 9. Predicted changes in carbon fluxes: (i) NPP, (ii) R_H , and (iii) NEP for all land areas north
 957 of 45 °N in response to transient climate change under the RCP 8.5 scenario (left panel) and RCP
 958 2.6 scenario (right panel) with dormancy model and MIC-TEM, respectively. The decadal running
 959 mean is applied.

960

961

962

963

964

965

966

967

968

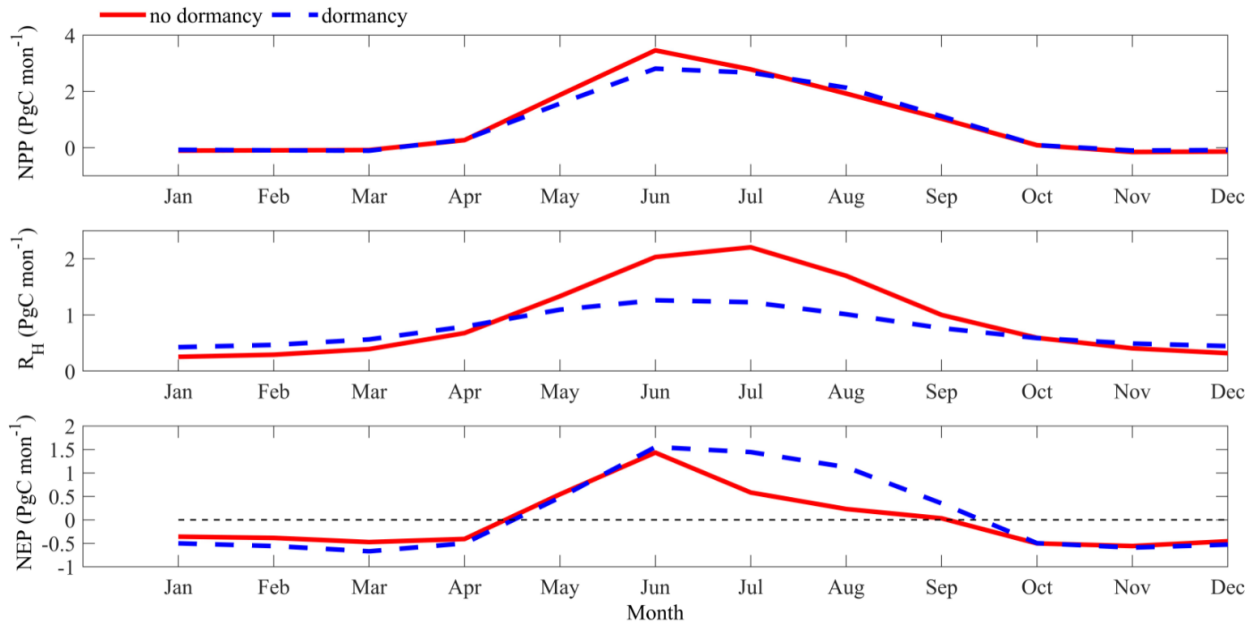
969

970

971

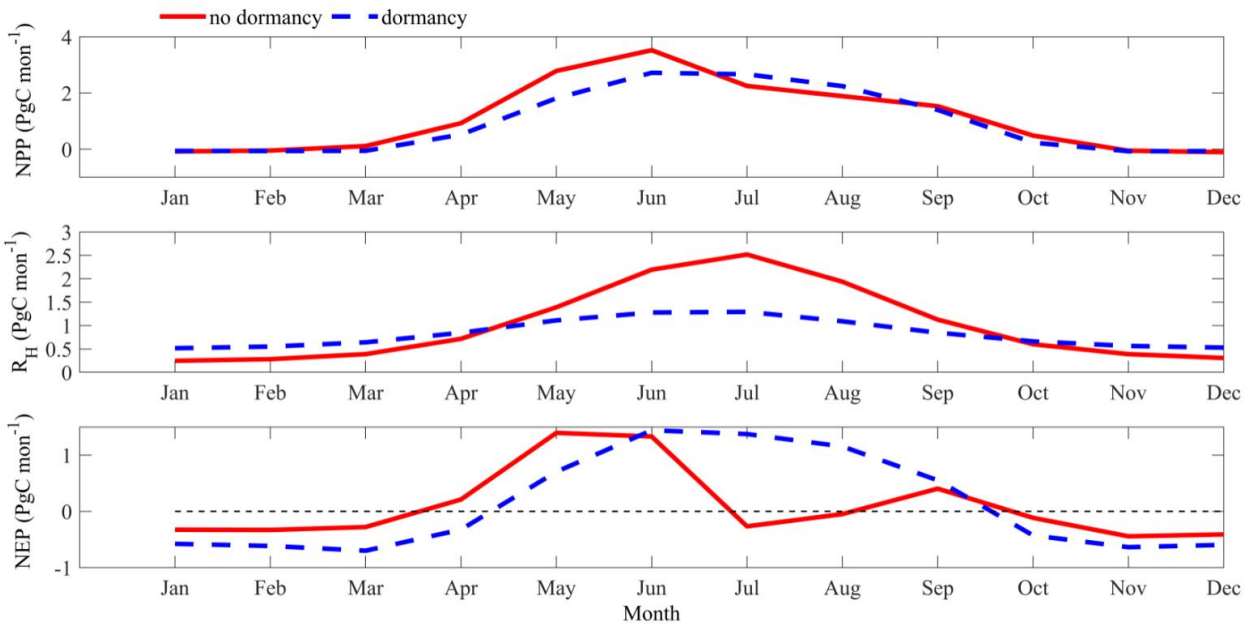
972

973 (a)



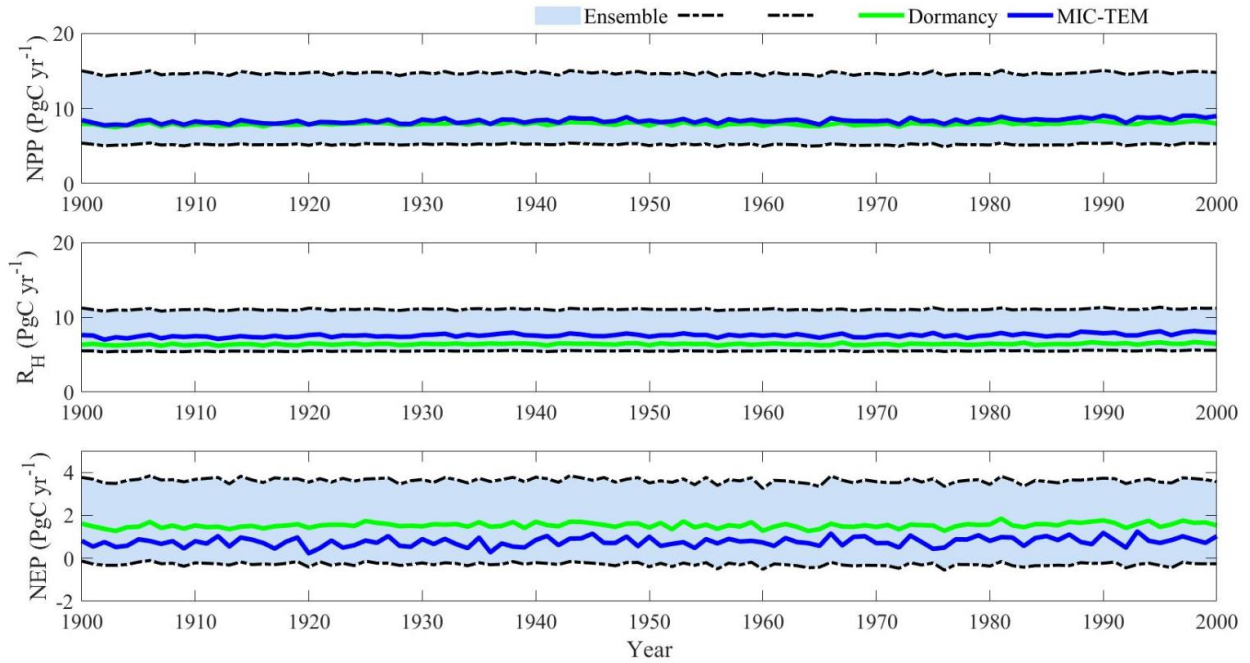
974

975 (b)



976

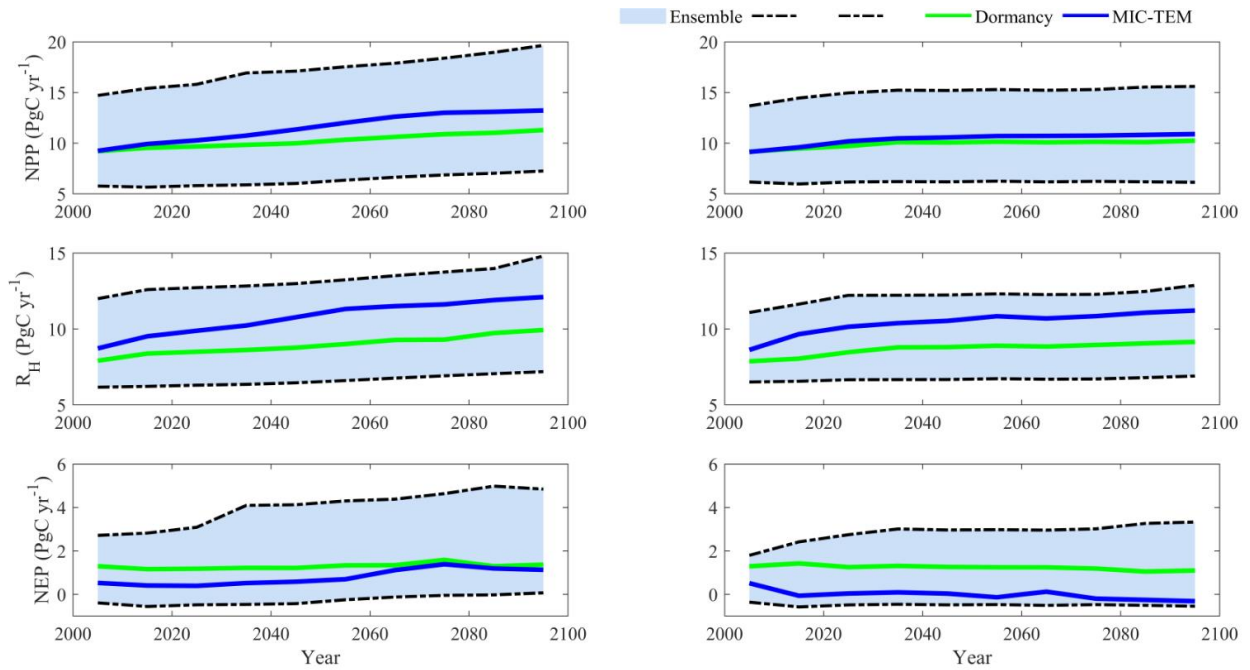
977 Figure 10. Regional annual seasonal pattern of simulated net primary production (NPP, top
978 panel), heterotrophic respiration (R_H , center panel) and net ecosystem production (NEP, bottom
979 panel) during the 2090s from dormancy model and MIC-TEM under: (a) RCP 2.6 scenario (top
980 panel) and (b) RCP 8.5 scenario (bottom panel). The region is all land areas north of 45 °N.
981



982
983

984 Figure 11. Simulated annual net primary production (NPP, top panel), heterotrophic respiration
985 (R_H , center panel) and net ecosystem production (NEP, bottom panel) by MIC-TEM-dormancy
986 with ensemble of parameters.

987
988
989
990
991
992
993
994
995
996
997
998
999
1000
1001
1002
1003
1004
1005
1006
1007
1008
1009
1010



1011
 1012
 1013
 1014
 1015
 1016
 1017
 1018

Figure 12. Simulated annual net primary production (NPP, top panel), heterotrophic respiration (R_H , center panel) and net ecosystem production (NEP, bottom panel) under RCP 8.5 scenario (left panel) and RCP 2.6 scenario (right panel) by MIC-TEM-dormancy with ensemble of parameters. The decadal running mean is applied. The grey area represents the upper and lower bounds of simulations.

1019 **Table 1. Parameters associated with detailed microbial dormancy in MIC-TEM-dormancy**
 1020

parameter	unit	description	Parameter range	references
m_R	h^{-1}	Specific maintenance rate at active state	[0.001, 0.08]	Wang et al. (2014)
Q_{10mic}	-	Temperature effects on microbial metabolic activity (rate change per 10 °C increase in temperature). Based on 0.65 eV activation energy for soils	[1.5, 3.5]	He et al. (2015)
Q_{10enz}	-	Temperature effects on enzyme activity (rate change per 10 °C increase in temperature). Based on 6% rate increase per degree Celsius	1.79	He et al. (2015)
α	-	the ratio of m_R to the sum of maximum specific growth rate	[0.01, 0.5]	Wang et al. (2014)
β	-	Ratio of dormant microbial maintenance rate to m_R	[0.0005, 0.005]	Wang et al. (2014)
Y_g	-	carbon use efficiency	[0.3, 0.7]	He et al. (2015)
K_s	$mgC\ cm^{-2}$	Half-saturation constant for directly accessible substrate	[0.01, 10]	Wang et al. (2014)
$K_{muptake}$	$mgC\ cm^{-2}$	Half-saturation constant for enzymatic decay of SOC	[200, 1000]	He et al. (2015)
r_{death}	h^{-1}	Potential rate of microbial death	$[2e^{-4}, 2e^{-3}]$	Allison et al. (2010)
$r_{EnzProd}$	h^{-1}	Enzyme production rate of microbe	$[1e^{-4}, 8e^{-4}]$	He et al. (2015)
$r_{enzloss}$	h^{-1}	Enzyme loss rate	[0.0005, 0.002]	Allison et al. (2010)
V_{max}	$mgC\ cm^{-2}\ h^{-1}$	Maximum SOC decay rate	$[1e^{-4}, 5e^{-3}]$	He et al. (2015)

1021
 1022
 1023

1024 **Table 2. Site description and measured NEP data used to calibrate MIC-TEM-dormancy**

Site Name	Location (Longitude (degrees) /Latitude (degrees))	Elevation (m)	Vegetation type	Description	Data range	Citations
Univ. of Mich. Biological Station	84.71W 45.56 N	234	Temperate deciduous forest	Located within a protected forest owned by the University of Michigan. Mean annual temperature is 5.83° C with mean annual precipitation of 803mm	01/2005- 12/2006	Gough et al. (2013)
Howland Forest (main tower)	68.74W 45.20N	60	Temperate coniferous forest	Closed coniferous forest, minimal disturbance.	01/2004- 12/2004	Davidson et al. (2006)
UCI-1964 burn site	98.38W 55.91N	260	Boreal forest	Located in a continental boreal forest, dominated by black spruce trees, within the BOREAS northern study area in central Manitoba, Canada.	01/2004- 10/2005	Goulden et al. (2006)
KUOM Turfgrass Field	93.19W 45.0N	301	Grassland	A low-maintenance lawn consisting of cool-season turfgrasses.	01/2006- 12/2008	Hiller et al. (2011)
Atqasuk	157.41W 70.47N	15	Wet tundra	100 km south of Barrow, Alaska. Variety of moist-wet coastal sedge tundra, and moist-tussock tundra surfaces in the more well-drained upland.	01/2005- 12/2006	Oechel et al. (2014);
Ivotuk	155.75W 68.49N	568	Alpine tundra	300 km south of Barrow and is located at the foothill of the Brooks Range and is classified as tussock sedge, dwarf-shrub, moss tundra.	01/2004- 12/2004	McEwing et al. (2015)

1025
1026
1027
1028

1029 **Table 3. Site description and measured NEP data used to validate MIC-TEM-dormancy**

1030

Site Name	Location (Longitude (degrees) /Latitude (degrees))	Elevation (m)	Vegetation type	Description	Data range	Citations
Bartlett Experimental Forest	71.29W/ 44.06N	272	Temperate deciduous forest	Located within the White Mountains National Forest in north-central New Hampshire, USA, with mean annual temperature of 5.61 °C and mean annual precipitation of 1246mm.	01/2005- 12/2006	Jenkins et al. (2007); Richardson et al. (2007);
Howland Forest (main tower)	68.74W/ 45.20N	60	Temperate coniferous forest	Closed coniferous forest, minimal disturbance.	01/2003- 12/2003	Davidson et al. (2006)
UCI-1964 burn site	98.38W/ 55.91N	260	Boreal forest	Located in a continental boreal forest, dominated by black spruce trees, within the BOREAS northern study area in central Manitoba, Canada.	01/2002- 12/2003	Goulden et al. (2006)
Brookings	96.84W/ 44.35N	510	Grassland	Located in a private pasture, belonging to the Northern Great Plains Rangelands, the grassland is representative of many in the north central United States, with seasonal winter conditions and a wet growing season.	01/2005- 12/2006	Gilmanov et al. (2005)
Atqasuk	157.41W/ 70.47N	15	Wet tundra	100 km south of Barrow, Alaska. Variety of moist-wet coastal sedge tundra, and moist-tussock tundra surfaces in the more well-drained upland.	01/2003- 12/2004	Oechel et al. (2014);
Ivotuk	155.75W/ 68.49N	568	Alpine tundra	300 km south of Barrow and is located at the foothill of the Brooks Range and is classified as tussock sedge, dwarf-shrub, moss tundra.	01/2005- 12/2005	McEwing et al. (2015)

1031

1032 **Table 4. Site description and measured R_H data used to validate MIC-TEM-dormancy model**

1033
1034
1035
1036
1037
1038
1039
1040
1041
1042
1043
1044

Site	Location (Longitude (degrees) /Latitude (degrees))	Elevation (m)	Vegetation type	Data range	Citations
US-EML	149.25W/ 63.88N	700	Alpine tundra	01/2009- 12/2013	Belshe et al. (2012)
CA-SJ2	104.65W/ 53.95N	580	Boreal forest	01/2004- 12/2008	Coursolle et al. (2006)
US-Ho2	68.75W/ 45.21N	91	Temperate coniferous forest	01/2000- 12/2004	Davidson et al. (2006)
US-UMB	84.71W/ 45.56N	234	Temperate deciduous forest	01/2005- 12/2006	Gough et al. (2013)
US-Ro4	93.07W/ 44.68N	274	Grasslands	01/2016- 12/2017	Griffis et al. (2011)
RU-Che	161.34E/ 68.61N	6	Wet tundra	01/2002- 12/2005	Merbold et al. (2009)

1045 **Table 5. Model validation statistics for Dormancy model and MIC-TEM at six sites with NEP data**

1046

1047

1048

1049

1050

1051

1052

1053

1054

1055

1056

1057

1058

1059

1060

1061

Site Name	Vegetation type	Models	Intercept	Slope	R-square	Adjusted R-square	p-value
Ivotuk	Alpine tundra	MIC-TEM	0.85	0.83	0.70	0.67	<0.001
		Dormancy	-0.51	1.09	0.75	0.73	<0.001
UCI-1964 burn site	Boreal forest	MIC-TEM	0.18	1.03	0.912	0.9080	<0.001
		Dormancy	-0.21	0.96	0.90	0.894	<0.001
Howland Forest (main tower)	Temperate coniferous forest	MIC-TEM	7.29	0.72	0.85	0.83	<0.001
		Dormancy	0.27	1.05	0.89	0.88	<0.001
Bartlett Experimental Forest	Temperate deciduous forest	MIC-TEM	-6.05	0.91	0.944	0.941	<0.001
		Dormancy	-2.34	1.13	0.93	0.924	<0.001
Brookings	Grassland	MIC-TEM	3.05	0.71	0.84	0.83	<0.001
		Dormancy	0.17	0.95	0.90	0.898	<0.001
Atqasuk	Wet tundra	MIC-TEM	7.22	1.85	0.71	0.70	<0.001
		Dormancy	0.19	0.82	0.67	0.66	<0.001

1062 **Table 6. Model validation statistics for Dormancy model and MIC-TEM at six sites with R_H data**
 1063

Site ID	Vegetation type	Models	Intercept	Slope	R-square	Adjusted R-square	RMSE	p-value
US-EML	Alpine tundra	MIC-TEM	2.90	0.91	0.79	0.78	3.55	<0.001
		Dormancy	1.81	0.74	0.87	0.85	2.69	<0.001
CA-SJ2	Boreal forest	MIC-TEM	7.59	1.12	0.84	0.83	9.8	<0.001
		Dormancy	2.6	0.74	0.86	0.85	3.97	<0.001
US-Ho2	Temperate coniferous forest	MIC-TEM	4.07	0.89	0.86	0.84	12.39	<0.001
		Dormancy	6.59	0.71	0.91	0.89	11.83	<0.001
US-UMB	Temperate deciduous forest	MIC-TEM	-4.73	1.32	0.81	0.8	20.05	<0.001
		Dormancy	13.6	0.67	0.85	0.84	12.94	<0.001
US-Ro4	Grassland	MIC-TEM	9.34	0.87	0.81	0.79	11.25	<0.001
		Dormancy	4.81	0.65	0.86	0.84	9.21	<0.001
RU-Che	Wet tundra	MIC-TEM	2.5	0.67	0.72	0.71	6.24	<0.001
		Dormancy	1.96	0.77	0.81	0.79	5.95	<0.001